Macroscopic modeling and numerical simulation of the return to liquid-vapor equilibrium

Matthieu Ancellin
Student at the École Centrale Paris
(Grande Voie des Vignes, Châtenay-Malabry, France),
during an internship at the
Centre de Mathématiques et de Leurs Applications
(École Normale Supérieure de Cachan et CNRS UMR8536
61 Avenue du Président Wilson, 94235 Cachan Cedex, France).

June - September 2011
Last revision of the document: February 13, 2013

Abstract

The object is to describe the reaction to excitation by a piston of a liquid-vapor system in the vicinity of the saturation curve. The return to thermodynamic equilibrium of a system out of equilibrium in a vessel of constant volume will first be studied. The model will then be extended to the case of an oscillating piston. Following a review of existing models, it was decided to model exchanges of matter and energy at the liquid-vapor interface using non-equilibrium thermodynamic equations. The differential equation systems obtained are solved numerically and the results presented and interpreted.

Contents

Part I

Constant volume

Chapter 1

Description of the system

1.1 Presentation of the problem

System

A closed adiabatic vessel is considered of height z. At the bottom of the vessel is a liquid (a pure substance such as water or methane) to a given height b, at a temperature T_l. The remainder of the vessel is filled by the same substance in gaseous form, at a pressure P_g and at a temperature T_g.

Hypotheses

a. The system is presumed to be invariant by translation perpendicular to z; the extensive values considered will be, unless indicated to the contrary, values per surface unit.

b. The temperature and pressure are presumed to be homogeneous within each of the two phases.

c. The gas will be modeled by an ideal gas with ideal gas law $P_g V = nRT_g$.

d. Liquid surface tension phenomena have not been taken into consideration (for further detail see section B.2).

Problem

At the initial point in time, the liquid-vapor system is not in a state of equilibrium ($P \neq P_{\text{sat}}(T)$ and/or $T_g \neq T_l$). Our objective in this part is to model the evolution of the system during relaxation which will bring it to a state of equilibrium.

Care will be taken in particular to ensure conservation of mass and energy during the course of relaxation.

Unless otherwise indicated, water will be considered throughout the remainder of the document.

1.2 Variables and notations

NB A table summarizing most of the notations is provided on page 61.

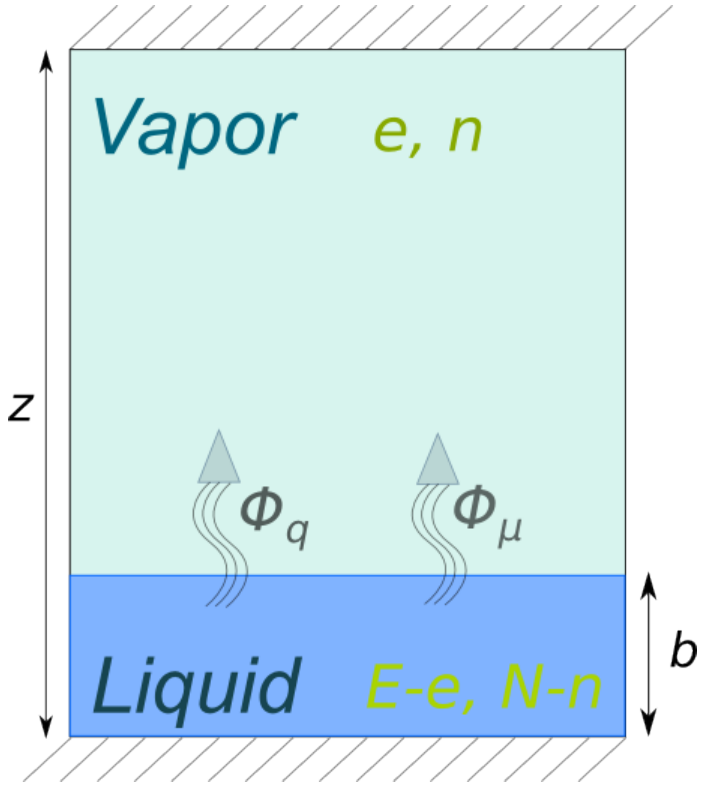

Figure 1.1: Diagram of the system studied

1.2.1 Variables

Definition By focusing our study on the energy aspect of the system, we were led to consider the following thermodynamic values, which entirely characterize the system and its state at a given point in time:

n Quantity of matter in the gas phase (in moles)

N Total quantity of matter in the liquid and gas phases (in moles)

e Internal energy of the gas phase

E Total internal energy (liquid and gas phases)

z Total height of the system

In the second part, we will introduce the sixth variable $\dot{z}$ to describe the system of differential equations as a first-order system. We will not consider $\dot{z}$ in this first part.

Quantity of matter The quantity of matter is used (measured in moles) to express the conservation of matter. In an equivalent way, one could use the mass of gas m and the total mass M as variables. It would simply require multiplication by the molar mass of all the expressions in which n and N occur.

Energy scale The absolute energy of the system does not appear in our problem, only variations in energy are relevant. The variables e and E will therefore describe differences in energy in relation to a reference state. (The notations e and E will be retained rather than ΔU_g and ΔU_{tot} only with a view to concision in the mathematical expressions.)

A reference state has thus been selected to work with. This state may be the initial state or the final state of equilibrium (if this is known *a priori*).

$\mathcal{E}^g_{ref}$ is defined as the molar energy of the gas at temperature T_{ref} and $\mathcal{E}^l_{ref}$ is the molar energy of the liquid at T_{ref}. They are linked (if the reference state is on the saturation curve) by

$$\mathcal{E}^g_{ref} - \mathcal{E}^l_{ref} = \mathcal{L}_{\text{vap}} \tag{1.1}$$

where $\mathcal{L}_{\text{vap}}$ is the latent vaporisation energy[1]. $\mathcal{E}^g_{ref}$ can be taken to $= 0$ and $\mathcal{E}^l_{ref}$ to $= -\mathcal{L}_{\text{vap}}$.

(1.1) can be interpreted as follows: at a fixed temperature, a mole of gas has an internal energy greater than that of a mole of liquid at the same temperature. This variance in energy is the latent heat that must be provided to the liquid for it to change to the gas state.

[1] If the reference state is outside the saturation curve, the two energies can be linked by $\mathcal{E}^g_{ref} - \mathcal{E}^l_{ref} = \mathcal{L}_{\text{vap}} + (C_g - C_l)(T_{ev}(P_{ref}) - T_{ref})$ where $T_{ev}(P)$ is the evaporation temperature at pressure P.

1.2.2 Other thermodynamic values

Other thermodynamic values characterizing the system are expressed on the basis of the five previous variables and physical constants for the chemical in question:

$$T_g(e, E, n, N, z) = T_{ref} + \frac{1}{\mathcal{C}_g}\left(\frac{e}{n} - \mathcal{E}^g_{ref}\right), \tag{1.2a}$$

$$T_l(e, E, n, N, z) = T_{ref} + \frac{1}{\mathcal{C}_l}\left(\frac{E-e}{N-n} - \mathcal{E}^l_{ref}\right), \tag{1.2b}$$

$$b\,(e, E, n, N, z) = \frac{(N-n)\mathcal{M}}{\rho_l}, \tag{1.2c}$$

$$P_g(e, E, n, N, z) = nR\frac{T_g(e, n)}{z - b(e, n)}, \tag{1.2d}$$

where T_g and P_g are the temperatures and pressure in the gas phase, T_l is the temperature of the liquid phase, b is the depth of the liquid phase.

$\mathcal{C}_g$ and $\mathcal{C}_l$ are the molar heat capacities at a constant volume of the gas and liquid phases (presumed to be constant), $\mathcal{M}$ is the molar mass of the chemical in question, ρ_l the density of the liquid (presumed to be constant) and R is the gas constant.

Pressure of the liquid The pressure of the liquid in the proximity of the surface is taken to be equal to the pressure of the vapor $P_l = P_g$ (see also section B.2). The pressure of the liquid far from the surface does not occur in this model.

1.2.3 Equilibrium vapor pressure

Several expressions exist for the equilibrium vapor pressure function (or saturation vapor pressure) $P_{\text{sat}}(T)$.

Antoine's law is expressed

$$P_{\text{sat}}(T) = P_{atm}\ \exp\left(A - \frac{B}{T + C}\right) \tag{1.3a}$$

where A, B et C are experimental coefficients. Numerical values are given, for example in table 3.1.

Clapeyron's relation is expressed

$$P_{\text{sat}}(T) = P_{ref}\ \exp\left(\frac{\Delta_{vap}\mathcal{H}}{R}\left(\frac{1}{T_{ref}} - \frac{1}{T}\right)\right). \tag{1.3b}$$

where $\Delta_{vap}\mathcal{H}$ is the latent vaporisation enthalpy.

This will be used in proximity with a point (P_{ref}, T_{ref}) on the saturation curve.

Comment One can also express

$$P_{\text{sat}}(T) = P_{ref} \exp\left(\frac{\gamma}{(\gamma-1)Ja}\left(1 - \frac{T_{ref}}{T}\right)\right) \tag{1.3c}$$

where Ja is the Jakob number and γ is the heat capacity ratio.

However in figure 1.2 we observe significant differences between these expressions

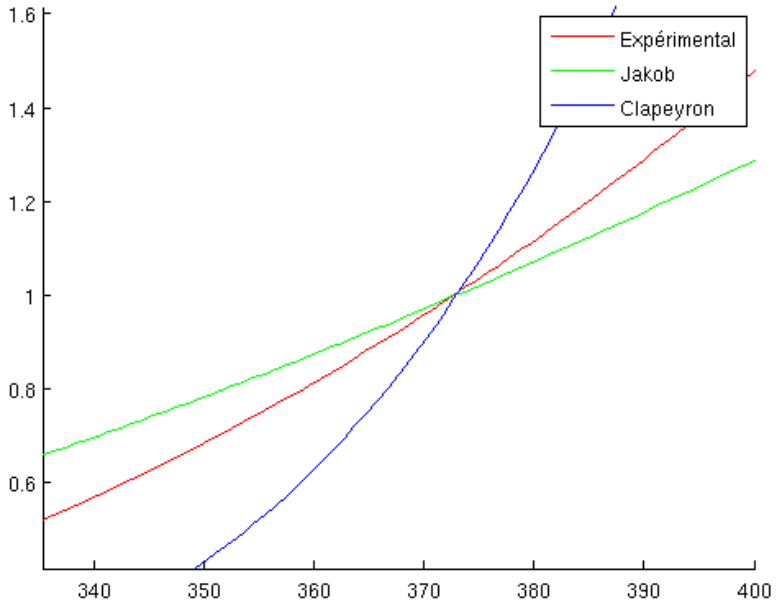

Figure 1.2: Three expressions of saturation pressure in the proximity of 370 K.
In red: Antoine's law (1.3a) with the numerical values of table 3.1 ;
in blue: Clapeyron's relation (1.3b) ;
in green: equation (1.3c) as used on the old phase change model.

1.2.4 Regarding the energy/enthalpy choice

In this first part we consider a constant volume system. For this reason, it seems more natural to use the *internal energy* rather than *enthalpy*[2].

Unless stated otherwise, the latent heat $\mathcal{L}_{\text{vap}}$ therefore refers to internal molar energy gained or lost during phase change.

[2]This choice is extended in the second part, where the system is no longer a fixed volume or fixed pressure system.

The internal molar energy of the gas can be expressed in molar enthalpy by:

$$\begin{aligned} \mathcal{H}^g &= \mathcal{E}^g + P\mathcal{V} \\ \Rightarrow \mathcal{H}^g &= \frac{e}{n} + RT_g \\ \Rightarrow \mathcal{H}^g &= \frac{e}{n}\left(1 + \frac{R}{\mathcal{C}_g}\right) + RT_{ref} \end{aligned} \tag{1.4}$$

where e is the energy of n moles of gas, and $\mathcal{H}$ the molar enthalpy of the gas. Here we took $\mathcal{E}^g_{ref} = 0$.

1.3 Dynamic of the system

1.3.1 Differential equations

The evolution of the system is governed by two main equations:

$$\frac{d}{dt}n = \Phi_\mu(e,n) \qquad \frac{d}{dt}e = \Phi_q(e,n) \tag{1.5a}$$

where Φ_μ and Φ_q are fluxes of matter and energy exchanged between the two elements of the system. These will be defined in the next chapter[3].

Three other differential equations implicitly complete this system:

$$\frac{d}{dt}N = 0 \qquad \frac{d}{dt}E = 0 \qquad \frac{d}{dt}z = 0 \tag{1.5b}$$

As such, they provide the conservation of energy and matter in the system. They can subsequently be modified to take into account a movement of the piston or a leak of thermal energy.

1.3.2 Initial conditions

Five parameters describe the system at the initial point in time: : (e_0, n_0, E, N, z).

In an equivalent manner one can consider the initial conditions $(P_0^g, T_0^g, T_0^l, b_0, z)$ as being more "natural". The first are deduced from the second (or vice versa) through the resolution of the following system:

$$n_0 = \frac{P_0^g(z - b_0)}{RT_0^g}, \tag{1.6a}$$

$$e_0 = n_0(\mathcal{C}_g(T_0^g - T_{ref}) + \mathcal{E}^g_{ref}), \tag{1.6b}$$

$$N = n_0 + \frac{b_0\rho_l}{\mathcal{M}}, \tag{1.6c}$$

$$E = e_0 + \frac{b_0\rho_l}{\mathcal{M}}(\mathcal{C}_l(T_0^l - T_{ref}) + \mathcal{E}^l_{ref}). \tag{1.6d}$$

Although the two sets of variables are equivalent, we will work here with the first of these, with which the differential equations (1.5) are expressed more easily.

[3] In practice, the relations in chapter 2 will give Φ_μ and $\Phi_q - \mathcal{H}^g\Phi_\mu$.

Chapter 2

Relaxation model

Appendix A presents a bibliographical study of liquid-vapor exchange models available in the literature. The findings from this are that the problem of theoretical expression of the flow of evaporation and condensation is not to date completely resolved. Many models exist, without it being possible to single out an expression that both conforms to experience and is devoid of empirical coefficient.

In this chapter, we will be studying more in detail the selected model of *Non-Equilibrium Thermodynamics* (NET).

2.1 Preliminary comments

a. All the theoretical and experimental work on the subject considers a non-equilibrium system but a stationary regime: for example, the same quantity of matter that evaporates every second is taken up in the vapor and re-injected into the liquid. This is, in effect, the mode of functioning of many industrial applications (evaporator, distiller). It is also in the stationary regime that precise experimental measurements can be made. It will be presumed that the relations obtained in the stationary regime are also valid in a transitory regime as is the case with ours.

b. A necessary hypothesis for the application of this model is that the system is in local equilibrium, even though it is not in global equilibrium. This signifies, in particular, that the usual thermodynamic values as well as the relations linking them, can be defined everywhere in the system. For a more extended discussion of local equilibrium, see [BK05].

2.2 Initial approach: Fick and Fourier

A fairly natural initial approach is to separate heat exchanges and exchanges of matter. A *Fourier law* (for the thermal aspect) is expressed side by side with a *Fick law* (for exchanges of matter). A system is obtained in the following form:

$$\frac{dn}{dt} = -D\Delta a, \qquad \frac{de}{dt} = -\lambda\Delta T \tag{2.1}$$

where D and λ are the diffusivity coefficients and a is the system's chemical activity.

Although it may provide satisfactory practical results, this system presents a major theoretical drawback: it does not respect the Onsager relations and is consequently in contradiction with the Second Principle of Thermodynamics [BK05, p.37]. Kjelstrup and Bedeaux [KB08, p. 6] cite errors of up to 20 to 30% in these cases and stress the importance of a more complete model.

Section 2.3 presents, fairly generally, some of the theoretical principles that we will subsequently apply in section 2.4 to obtain the equations for our fluxes.

2.3 Principles of non-equilibrium thermodynamics

Numerous works on thermodynamics or statistical physics set out in more or less detail the principles of non-equilibrium thermodynamics. One may refer to [Bal03] for further detail.

Comment

In this document we deal with the case of exchanges of two quantities (matter and energy) between two discrete overall groups. More general cases can of course be treated with the same formalism (exchange of N extensive values, a continuous collection of points, etc.). The Fourier, Ohm and Fick laws or Navier-Stokes equations can be seen as special cases of this general formalism [Bal03].

Associated extensive and intensive values

With the quantity of matter and energy, we associate respectively, the intensive variables $-\mu/T$ and $1/T$, where μ is the chemical potential and T temperature. The reason for this choice is the following equation,

$$dS = \frac{1}{T}dU - \frac{\mu}{T}dN. \tag{2.2}$$

Entropy, which here creates the relation between intensive and extensive variables, plays an important role in the theory of non-equilibrium thermodynamics.

Thermodynamic forces

Thermodynamic forces are defined as the gradients of the intensive values defined previously:

$$\Gamma_q = \frac{1}{T_g} - \frac{1}{T_l}, \qquad \Gamma_\mu = \frac{\mu_g}{T_g} - \frac{\mu_l}{T_l}. \tag{2.3}$$

Fluxes

Fluxes of matter and energy exchanged between the two phases are written, respectively, as Φ_μ and Φ_q.

Linear phenomenological relations

The heart of this formalism is the system of linear equations linking the fluxes (Φ) and forces (Γ)

$$\Phi_q = L_{qq}\Gamma_q + L_{q\mu}\Gamma_\mu \qquad \Phi_\mu = L_{\mu q}\Gamma_q + L_{\mu\mu}\Gamma_\mu \tag{2.4}$$

The coefficients L_{ij} can be called *transfer coefficients*, *response coefficients*, *Onsager coefficients* or *generalized conductances*. They may be dependent upon the thermodynamic values of the system, but are independent of the forces and the fluxes.

Creation of entropy

One may express the rate of entropy created, as:

$$\frac{d}{dt}S = \Phi_q\Gamma_q + \Phi_\mu\Gamma_\mu. \tag{2.5}$$

In the following section, we will use as a starting point the expression of $\frac{d}{dt}S$ to identify the forces and associated fluxes.

Onsager relation(s) ($\sim$ 1930)

The coupling terms are equal:

$$L_{q\mu} = L_{\mu q}. \tag{2.6}$$

The presence of coupling terms and their equality is a consequence of the Second Law of Thermodynamics.

This principle also involves the following inequalities:

$$L_{qq} \geq 0 \qquad L_{\mu\mu} \geq 0 \qquad L_{qq}L_{\mu\mu} \geq L_{q\mu}^2 \tag{2.7}$$

which flow directly from $\frac{d}{dt}S \geq 0$.

Generalised resistances

One may invert the linear system (2.4) to cause the R_{ij} coefficients to appear, referred to as *resistances* or *generalized resistances* :

$$\Gamma_q = R_{qq}\Phi_q + R_{q\mu}\Phi_\mu, \qquad \Gamma_\mu = R_{\mu q}\Phi_q + R_{\mu\mu}\Phi_\mu. \tag{2.8}$$

These coefficients verify the same Onsager relations cited above. In many studies, these are the coefficients that are used, calculated or measured instead of conductances.

2.4 Application to phase change

The reasoning that follows is based on the reasoning presented in a more or less fragmentary way in the multitude of documents covering NET cited in the bibliography. Many variants in these versions of reasoning may be noted, according to the complexity and model selected (surface temperature different from that of the gas for example) or values that will be calculated/measured (heat fluxes different in gas and in liquid).

A simple model has been selected here enabling the calculation of the terms of the equations (1.5a).

For further theoretical detail, see for example [BK05] or [KB08]

Fluxes

Φ_μ is defined as the flux of matter traversing the interface, Φ_q is the total flux of energy exchanged, Φ_q^g the "measurable flux of energy" in the gas phase, Φ_q^l the "measurable flux of energy" in the liquid phase. They are linked by the following identity:

$$\Phi_q = \Phi_q^l + \mathcal{H}^l \Phi_\mu = \Phi_q^g + \mathcal{H}^g \Phi_\mu \tag{2.9}$$

where $\mathcal{H}^i$ is the molar enthalpy of the phase i. Below in this document, the fluxes are counted positively where they move from l to g

Gibbs-Helmholtz

The following relation will be used:

$$\frac{\partial(\mu_i/T)}{\partial(1/T)} = \mathcal{H}^i \quad \Longrightarrow \quad \frac{\mu_i(T_1)}{T_1} = \frac{\mu_i(T_2)}{T_2} + \mathcal{H}^i\Big(\frac{1}{T_1} - \frac{1}{T_2}\Big) \tag{2.10}$$

A second order term in temperature difference is sometimes added. It is in the form $\frac{1}{2}\mathcal{C}_p^i(1 - T_1/T_2)^2$

Creation of entropy

Generally the starting point for the reasoning is expressing the level of creation of entropy at the interface. Roughly, this entails a chain derivation of S with the relations (2.2). For a more rigorous demonstration, see, for example [BK05].

$$\dot{s} = \Phi_q\Big(\frac{1}{T_g} - \frac{1}{T_l}\Big) + \Phi_\mu\Big(\frac{\mu_l(T_l)}{T_l} - \frac{\mu_g(T_g)}{T_g}\Big) \quad (\geq 0) \tag{2.11}$$

Rather than extracting the linear relations from these forces/fluxes pairs, we will transform the expression of $\dot{s}$ to obtain new force/flux pairs. The equations (2.9) and (2.10) give :

$$\dot{s} = \Phi_q^g\Big(\frac{1}{T_g} - \frac{1}{T_l}\Big) + \Phi_\mu \frac{\mu_l(T_l) - \mu_g(T_l)}{T_l} \tag{2.12}$$

Two reasons may justify this choice:

a. The flux Φ_q^g (as well as Φ_q^l) are the fluxes that are measured experimentally. For this reason, these are the ones that are the most often used in work on the subject. And it is the coefficients associated with this forces/fluxes pair that can be found in the bibliography.

b. The difference in chemical potentials at the same temperature is more easily expressed than the difference in potentials at different temperatures. The expression is given at (2.17).

Phenomenological relations

From (2.12), one can therefore derive:

$$\Phi_q^g = L_{qq}\Big(\frac{1}{T_g} - \frac{1}{T_l}\Big) + L_{q\mu}\frac{\mu_l(T_l) - \mu_g(T_l)}{T_l}, \tag{2.13a}$$

$$\Phi_\mu = L_{q\mu}\Big(\frac{1}{T_g} - \frac{1}{T_l}\Big) + L_{\mu\mu}\frac{\mu_l(T_l) - \mu_g(T_l)}{T_l}. \tag{2.13b}$$

Expression of the difference in chemical potentials

For the chemical potential of the gas, we have:

$$\mu_g(T_l) = \mu_g^0(T_l) + RT_l \ln\Big(\frac{P_g}{P_{ref}}\Big) \tag{2.14}$$

where μ_g^0 corresponds to the reference state of the vapor and P_{ref} is the reference pressure.

Similarly for the liquid, we have:

$$\mu_l(T_l) = \mu_l^0(T_l) + \frac{\mathcal{M}}{\rho_l}(P_l - P_{ref}). \tag{2.15}$$

Whereas, at the equilibrium $(T_l,\, P_{\text{sat}}(T_l))$, we would have $\mu_l(T_l) = \mu_g(T_l)$, hence:

$$\mu_l^0(T_l) - \mu_g^0(T_l) = RT_l \ln\Big(\frac{P_{\text{sat}}(T_l)}{P_{ref}}\Big) - \frac{\mathcal{M}}{\rho_l}(P_{\text{sat}}(T_l) - P_{ref}). \tag{2.16}$$

The previous three equations give:

$$\frac{\mu_l(T_l) - \mu_g(T_l)}{T_l} = R\ln\big(\frac{P_{\text{sat}}(T_l)}{P_g}\big) + \frac{\mathcal{M}}{\rho_l T_l}(P_l - P_{\text{sat}}(T_l)). \tag{2.17}$$

In practice, the second term is much smaller that the first ($\mathcal{M}/\rho_l T_l R \approx 10^{-8}$ Pa^{-1} for water). Only considering the term as a logarithm is good approximation. This will be seen numerically in section 3.4

Comparison with the bibliography

The same equations are found in [SBK+06], [XKB+06] and [GBSK07] (with sometimes fluxes counted in the reverse direction).

[BK99], [BK05] and [KB08] give the same expression for the relations (2.13), but [BK99] and [KB08] only retain the term in logarithm in (2.17) ([BK05] does not detail the difference in potentials).

2.5 Comments on the previous results

a. Two smaller terms can be added to the difference of chemical potentials:

$$\text{eq. (2.17)} \; + R \ln\Big(\frac{\phi_{sat}(T_l,P)}{\phi(T_l,P)}\Big) - \frac{1}{2}\mathcal{C}_p^g\Big(1-\frac{T_g}{T_l}\Big)^2 \tag{2.18}$$

The first term introduces the fugacity ϕ for a non-ideal gas model. The second is the term as the square of the temperature difference that we had disregarded in the Gibbs-Helmholtz relation (2.10).

b. Sometimes the interface is considered as a "third phase" capable of accumulating the energy and having its own temperature. As an alternative to the formulation (2.11), one may thus find the following formulation for the level of formation of entropy:

$$\dot{s} = \Phi_q^g\Big(\frac{1}{T_g}-\frac{1}{T_s}\Big) + \Phi_q^l\Big(\frac{1}{T_s}-\frac{1}{T_l}\Big) + \Phi_\mu\Big(\frac{\mu_l(T_s)}{T_s}-\frac{\mu_g(T_s)}{T_s}\Big) \tag{2.19}$$

where T_s is the temperature at the interface. It is noted that positing $T_s = T_l$ enables us to find the equation (2.12).

c. One can see that the fact emerges that in our model, the latent heat $\mathcal{L}_{\text{vap}}$ is removed or returned in the energy of the liquid phase. This is naturally an approximation. It would be more rigorous to remove and return this energy in the energy of the interface (T_s), which would then return to the thermal equilibrium through conductive exchanges with the gas and the liquid. We are implicitly positing the hypothesis here that thermal conduction is much easier between the liquid and the interface than between the gas and the interface and that in consequence, the interface and the liquid can be merged.

d. Symmetrically, one could consider the following relations, equivalent to (2.13) and which are obtained using a similar reasoning.

$$\Phi_q^l = L_{qq}^l\Big(\frac{1}{T_g}-\frac{1}{T_l}\Big) + L_{q\mu}^l\frac{\mu_l(T_g)-\mu_g(T_g)}{T_g}, \tag{2.20a}$$

$$\Phi_\mu = L_{\mu q}^l\Big(\frac{1}{T_g}-\frac{1}{T_l}\Big) + L_{\mu\mu}^l\frac{\mu_l(T_g)-\mu_g(T_g)}{T_g}, \tag{2.20b}$$

with

$$\frac{\mu_l(T_g)-\mu_g(T_g)}{T_g} = R\ln\Big(\frac{P_{\text{sat}}(T_g)}{P_g}\Big) + \frac{\mathcal{M}}{\rho_l T_g}(P_l - P_{\text{sat}}(T_g)). \tag{2.21}$$

e. The coefficients L_{ij}^l from the equations (2.20) are not equal to the coefficient L_{ij} (which could be renamed L_{ij}^g) from the equations (2.13). Regarding the relations linking L_{ij}^l and L_{ij}^g, see [KB08] or [SBK+06, eq. (23)]

f. In all cases, it is indeed verified that:

$$T_g = T_l \;\text{ et }\; P_g = P_{\text{sat}}(T_g) \;\Longrightarrow\; \Phi_\mu = 0 \;\text{ et }\; \Phi_q = 0$$

2.6 Transfer coefficients

The coefficients linking the forces and fluxes in a linear manner in the phenomenological relations of the non-equilibrium thermodynamic are the most problematic points of this model. In the following paragraphs we will study these in more detail and compare the different expressions that may be used.

Dimensional analysis

In our model, we have:

$$L_{qq} \equiv [kg \cdot K \cdot s^{-3}] \equiv [W \cdot K \cdot m^{-2}], \tag{2.22a}$$
$$L_{q\mu} \equiv [mol \cdot K \cdot s^{-1} \cdot m^{-2}], \tag{2.22b}$$
$$L_{\mu\mu} \equiv [mol^2 \cdot K \cdot s \cdot kg^{-1} \cdot m^{-4}] \equiv [mol^2 \cdot K \cdot J^{-1} \cdot s^{-1} \cdot m^{-2}]. \tag{2.22c}$$

Other variants are possible, according to whether one is working in 1D or not and for mass, molar or molecular quantities.

In some documents, there are coefficients of the type $L'_{ij} = L_{ij}/T_s$ or L_{ij}/T_l whose dimension therefore does not entail the involvement of K.

Unless otherwise indicated, throughout the remainder of the document, coefficients will be expressed in the units presented in (2.22) even though they are not explicitly written.

2.6.1 According to kinetic theory

Study of the kinetic theory of the gasses enables the calculation of the expressions for these coefficients. These coefficients are calculated for mono-atomic gasses in the vicinity of the triple point

Expressions

Although they sometimes express coefficients in a slightly different way, [BK99, p. 420], [RKBH01, p. 357], [JB04, p. 261] or even [XKB+06, p. 455] agree on the following lines:

$$R_{qq} = \frac{\sqrt{\pi}(1 + {}^{104}/_{25\pi})}{4c^g R T_g^2 v_{mp}}, \tag{2.23a}$$
$$R_{q\mu} = R_{\mu q} = \frac{\sqrt{\pi}(1 + {}^{16}/_{5\pi})}{8c^g T_g v_{mp}}, \tag{2.23b}$$
$$R_{\mu\mu} = \frac{2R\sqrt{\pi}({}^{1}/_{\sigma} + {}^{1}/_{\pi} - {}^{23}/_{32})}{c^g v_{mp}}, \tag{2.23c}$$

$$\text{with} \quad v_{mp} = \sqrt{\frac{3RT^g}{\mathcal{M}}} \quad \text{and} \quad c^g = \frac{n}{z - b}$$

where R_{ij} are the resistances defined in the relation (2.8), c^g is the molar density of the gas, v_{mp} the most probably speed of the particles, R is the gas constant and σ is the empirical evaporation coefficient also referred to in A.1.

Values of σ between 0.1 and 1 are generally used.

Comments

a. In all the documents cited above, it seems implicit that these coefficients are those that correspond to the coefficients (referred to previously as L_{ij}^g) linking Φ_q^g to the other magnitudes. a. See in particular the comments at d. and e. in section 2.5.

b. Johannessen et al. [JB04, p. 261] (and others) evaluate the coefficients at the surface temperature and not at the temperature of the gas. In our model, it would be necessary to take the temperature of the liquid T_l. This would not change the orders of magnitude.

c. This formulation still entails the involvement of the empirical parameter σ, whose value remains under discussion. It only seems to be involved for the transfer of mass in the expressions above but the transition from resistances to conductances means that it is involved in all the L_{ij} coefficients.

Orders of magnitude

For the initial conditions of the type as used in chapter 3.1 ($T \sim 370$ K), we find the following orders of magnitude:

$$\sigma = 0.1 : \quad L_{qq} \sim 10^{10} \quad L_{q\mu} = L_{\mu q} \sim -10^5 \quad L_{\mu\mu} \sim 10 \text{ to } 10^2 \tag{2.24a}$$

$$\sigma = 1 : \quad L_{qq} \sim 10^{10} \quad L_{q\mu} = L_{\mu q} \sim -10^6 \quad L_{\mu\mu} \sim 10^3 \tag{2.24b}$$

where the units are those presented above in the equations (2.22).

In the vicinity of the triple point, the coefficients are 5 to 10 times weaker.

The Onsager relations for these coefficients are indeed verified. The coupling terms here represent approximately 5 to 20 % of the direct terms.

Validity

Although practical to use, the validity of these coefficients has often been called into question in experimental tests (whether actual or numerical – a review of some of these tests is found in section A.3). In particular, the use of these coefficients for non-mono-atomic particles far from the triple point seems hazardous.

It would seem that similar calculations exist for molecular gasses, but that "convenient expression are not available" [BK99, p. 420]...

2.6.2 Experimental

In Table 2.1, we report some of the values obtained by the Fang and Ward experiments [FW99b] (used in [BK99]) and by Badam et al. [BKDD07]. These values may serve as a comparison with the other expressions or directly in a numerical simulation.

Coupling coefficients The experimental data enable the calculation of only two coefficients out of three. A hypothesis is required to obtain numerical values.

	P_g (Pa)	T_l (°C)	T_g (°C)	L_{qq}	$L_{\mu\mu}$
[BK99] (water)	277	$-10,2$	$-4,1$	$1,34 \cdot 10^6$	$2,8 \cdot 10^{-2}$
[BK99] (octane)	350	$-1,1$	$3,7$	$7,47 \cdot 10^5$	$2,1 \cdot 10^{-4}$
[BK99] (C_7H_{14})	2037	$3,7$	$7,0$	$5,3 \cdot 10^5$	$3,0 \cdot 10^{-3}$
[BKDD07] (water)	490,0	$-2,96$	$-0,93$	$2,8 \cdot 10^6$	$1,5 \cdot 10^{-3}$
	483,0	$-3,18$	$1,04$	$3,6 \cdot 10^6$	$2,2 \cdot 10^{-3}$
	567,0	$-0,97$	$4,82$	$4,1 \cdot 10^6$	$1,2 \cdot 10^{-3}$
	569,2	$-0,92$	$7,86$	$4,3 \cdot 10^6$	$1,1 \cdot 10^{-3}$

Table 2.1: Some transfer coefficient values obtained experimentally for water, octane and methylcyclohexane (C_7H_{14}). The dimensions of the coefficients are those present in the equations (2.22).

For this the following relation is used, derived from kinetic theory

$$\frac{L_{q\mu}}{L_{\mu\mu}} = -k_h \mathcal{L}_{\text{vap}} \quad \text{with } k_h = 0.18$$

The chosen value of k_h has relatively little impact on the calculation of L_{qq}, but a very large influence on the values of $L_{\mu\mu}$ given in table 2.1.

Comments

a. The temperatures and pressures used here are below the triple point. We should not forget that the system is maintained in non-equilibrium so that the evaporation can take place and does not necessarily need to be in the vicinity of the saturation curve.

b. We note a variance of 2 to 4 orders of magnitude with the results of (2.24).

c. The ratio $L_{qq}/L_{\mu\mu}$ is of the same order of magnitude as in (2.24a). By construction, $L_{q\mu}/L_{\mu\mu}$ is also of the same order of magnitude as in the kinetic theory. One may therefore hold that the coefficients of kinetic theory will give good results up to a time scaling constant.

2.6.3 According to SRT

As cited in [BKDD07] and [BS04], the linearization of the SRT (see A.2) means that a coefficient $L_{\mu\mu}$ for the NET can be suggested. Expressed in the same dimensions as (2.22), we obtain :

$$L_{\mu\mu} = 2\frac{P_{\text{sat}}(T_l)}{R\sqrt{2\pi\mathcal{M}RT_l}} \exp\left(\frac{\mathcal{M}}{\rho_l RT_l}(P_{\text{sat}}(T_l) - P_l^e)\right) \tag{2.25}$$

where P_l^e is the pressure of the liquid in the equilibrium state.

Orders of magnitude

With the hypothesis that we are close to equilibrium, we may approach the exponential by 1. We obtain the following orders of magnitude.

$$T_l = 273\text{K}: \qquad L_{\mu\mu} \simeq 1.61 \cdot 10^2 \tag{2.26a}$$

$$T_l = 373\text{K}: \qquad L_{\mu\mu} \simeq 1.28 \cdot 10^3 \tag{2.26b}$$

In order of magnitude, these results are closed those of kinetic theory ($\sigma = 1$), and therefore fairly distant from experience.

2.7 Complete equations

We resume the relations from chapter 1. To these are added the equations (2.9), (2.13) and (2.17). We obtain :

$$\frac{de}{dt} = L_{qq}\Delta\frac{1}{T} + L_{q\mu}\Delta\frac{\mu}{T} + \mathcal{H}^g\frac{dn}{dt}, \tag{2.27a}$$

$$\frac{dn}{dt} = L_{q\mu}\Delta\frac{1}{T} + L_{\mu\mu}\Delta\frac{\mu}{T}, \tag{2.27b}$$

where

$$\Delta\frac{1}{T} = \frac{1}{T_{ref} + \frac{e}{\mathcal{C}_g n}} - \frac{1}{T_{ref} + \frac{1}{\mathcal{C}_l}\left(\frac{E-e}{N-n} + \mathcal{L}_{\text{vap}}\right)}, \tag{2.27c}$$

$$\Delta\frac{\mu}{T} = R\ln\left[\frac{P_{\text{sat}}\left[T_{ref} + \frac{1}{\mathcal{C}_l}\left(\frac{E-e}{N-n} + \mathcal{L}_{\text{vap}}\right)\right]\left(z - \frac{(N-n)\mathcal{M}}{\rho_l}\right)}{nR\left(T_{ref} + \frac{e}{\mathcal{C}_g n}\right)}\right], \tag{2.27d}$$

$$\mathcal{H}^g = \frac{e}{n}\left(1 + \frac{R}{\mathcal{C}_g}\right) + RT_{ref}, \tag{2.27e}$$

$$\text{and } P_{\text{sat}}(T) = P_{atm}\exp\left(A - \frac{B}{T-C}\right). \tag{2.27f}$$

Chapter 3

Numerical resolutions

3.1 Implementation

The transfer coefficients are those of the kinetic theory of gasses, as presented in the equation (2.23). We have arbitrarily taken $\sigma = 0.1$.

The numerical values of the constants ($\mathcal{C}_g$, $\mathcal{C}_l$, ...) are presented in table 3.1. The small approximations made on the value of these constants do not change the appearance of the results presented below. Unless otherwise stated, the tests are performed using the constants for water.

We have written the two differential equations (2.27) coupled in functions of the variables e and n defined in chapter 1, which will be resolved numerically with Matlab.

Magnitude	Water	Methane
$\mathcal{M}$ $(kg \cdot mol^{-1})$	$18 \cdot 10^{-3}$	$16 \cdot 10^{-3}$
$\mathcal{L}_{\text{vap}}$ $(J \cdot mol^{-1})$	$37.5 \cdot 10^{3}$	$8.1 \cdot 10^{3}$
$\mathcal{C}_g$ $(JK^{-1}mol^{-1})$	28	40
$\mathcal{C}_l$ $(JK^{-1}mol^{-1})$	75	55
ρ_l $(kg \cdot m^{-3})$	1000	416
P_{triple} (bar)	$6 \cdot 10^{-3}$	0,11
T_{triple} (K)	273	90
$P_{critique}$ (bar)	220	46
$T_{critique}$ (K)	647	190
P_{sat} A	5.083	3.98
B (K)	1663.12	443.0
C (K)	-45.62	-0.49

Table 3.1: Data used. The coefficients A, B and C are those of Antoine's law for pressure and saturation. Source : NIST (http://webbook.nist.gov/chemistry/)

3.2 Influence of the initial conditions on the results

3.2.1 Case 1. – Influence of P_0 and T_0^g

Initial conditions

In this case, we launched 4×4 initial conditions for pressures ranging from 90 kPa to 120 kPa in steps of 10 kPa and initial gas temperatures of between 362.5 K and 377.5 K in steps of 5 K. The total height, initial temperature of the liquid and initial fraction of the liquid were fixed, and their values were respectively $z_0 = 1$ m, $T_0^l = 370$ K and $b_0 = 0.01 \cdot z_0$.

Graphs

See Figures 3.1 and 3.2.

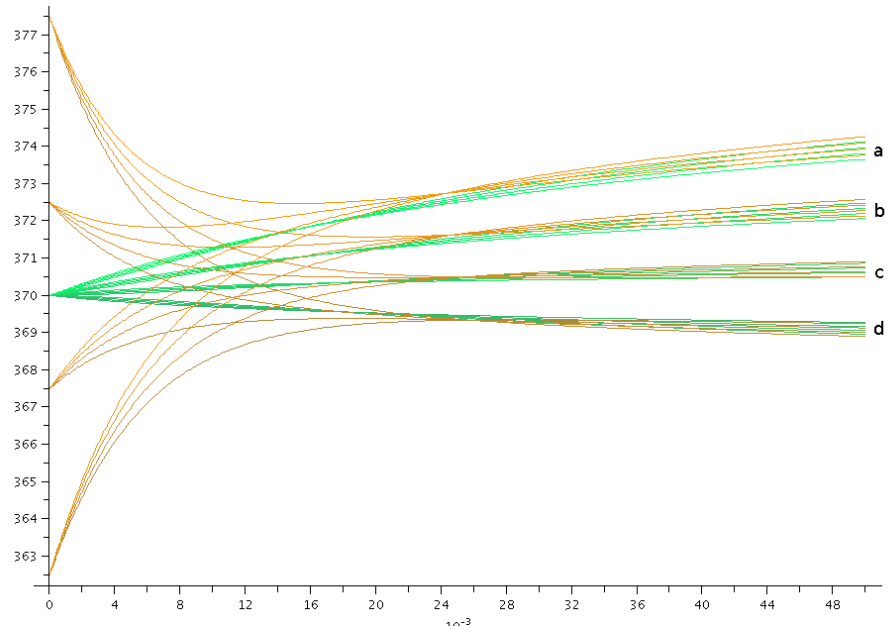

Figure 3.1: *Orange* is the temperature of the gas (K) and *green* is the temperature of the liquid (K) against time (s).
Case 1. $P_g = 90 + 10i$ kPa ($i \in [0, 3]$), $T_g = 362.5 + 5j$ K ($j \in [0, 3]$), $z_0 = 1$ m, $T_0^l = 370$ K and $b_0 = 0.01 \cdot z_0$

Interpretation

The line bundles (a), (b) and (c) are reductions in pressure, therefore condensations. Whereas the opposite is the case in (d) which is a vaporisation.

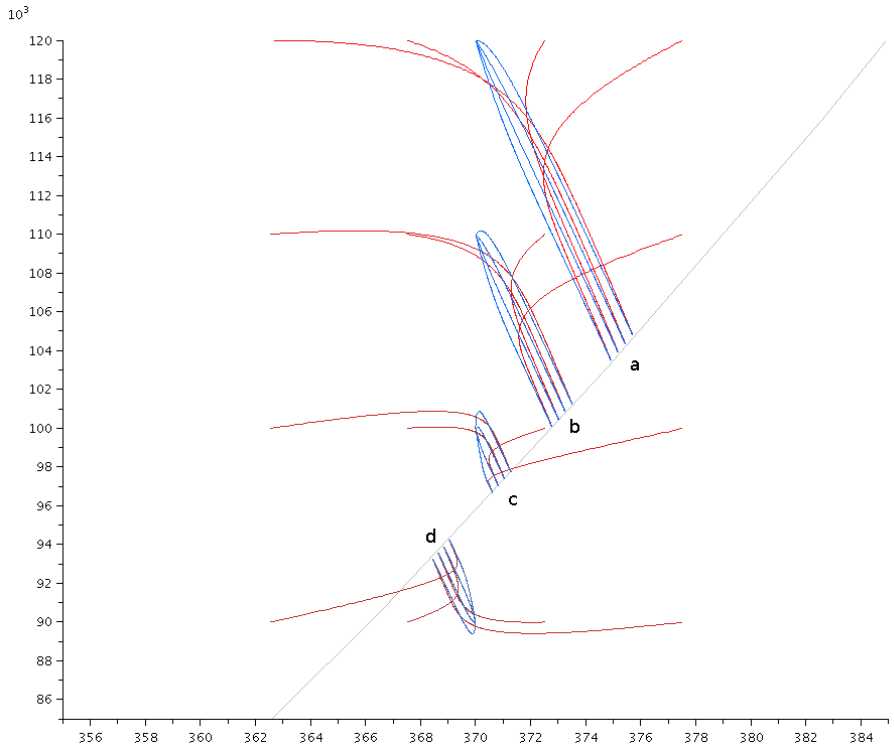

Figure 3.2: Pressure diagram (kPa) against temperature (K).
Red is the change from the gas phase, *blue* is the change from the liquid phase.
Grey is the saturation curve $P = P_{\text{sat}}(T)$.
Case 1. $P_g = 90 + 10i$ kPa ($i \in [0, 3]$), $T_g = 362.5 + 5j$ K ($j \in [0, 3]$), $z_0 = 1$ m, $T_0^l = 370$ K and $b_0 = 0.01 \cdot z_0$

In these simulations, where the liquid water represents 1% of the volume, but 95% of the quantity of matter, the most important criterion for determining the final state seems to be the initial gas pressure P_0^g.

A greater initial pressure leads to a greater final pressure.

More surprisingly, the inverse effect was observed for the initial temperature of the gas: at a fixed pressure a higher initial pressure leads to a lower final temperature.

The appearance of the curves shows two stages in the relaxation. Returns to chemical and thermal equilibrium occur within different timescales. In this case thermal equilibrium is the most rapid ($\sim$ 25 ms), whereas the liquid-vapor equilibrium is reached later ($\sim$ 200 ms).

3.2.2 Case 2. – Influence of the initial quantity of liquid

Initial conditions

We now vary the fraction of liquid in relation to the gas. The following table presents the values used. The other parameters are : $T_0^g = 360$ K, $T_0^l = 380$ K, $P_0 = 1$ bar and $z_0 = 1$ m.

Curve index	Fraction in volume	Fraction in quantity of matter
a	13 %	99.5 %
b	1.8 %	97 %
c	0.24 %	80 %
d	0.034 %	35 %
e	0.0045 %	7 %
f	0.00061 %	1 %

Graph

See Figure 3.3.

Interpretation

The final equilibrium state is strongly dependent on the quantity of liquid present initially. Even if the gap from the saturation curve is the same, the latent vaporisation energy has a different impact on the temperature according to the quantity of material (in our model, liquid) which will supply it/gain, and the system will therefore be oriented towards a different equilibrium state.

We have here two asymptotic cases:

- The curves (a) and (b) tend towards the case $n_{liquid} \gg n_{gas}$: the liquid operates as a thermostat, its temperature varies little, and it is this temperature that fixes the final state of the system. The gas pressure increases with the temperature and the increase in quantity of matter.
- The curves (e) and (f) tend towards the case $n_{liquid} \ll n_{gas}$. The pressure of the gas cannot reach equilibrium other than by increasing its temperature.

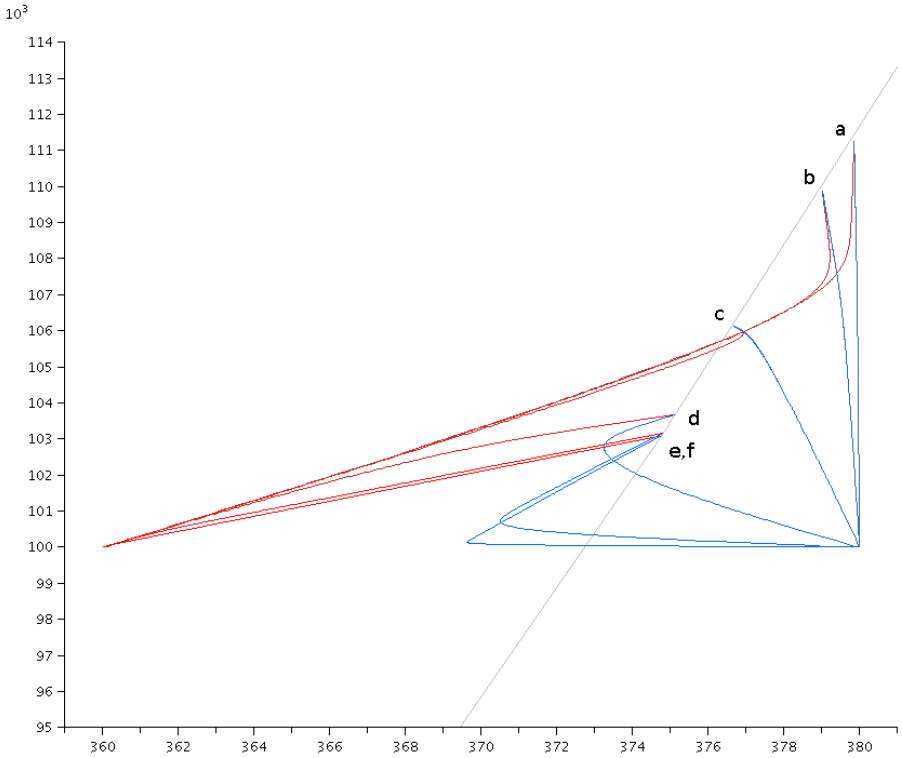

Figure 3.3: Pressure diagram (kPa) against (K). *Red* is the change from the gas phase, *blue* is the change from the liquid phase. *Grey* is the saturation curve $P = P_{\text{sat}}(T)$.
Case 2. $T_0^g = 360$ K, $T_0^l = 380$ K, $P_0 = 1$ bar, $z_0 = 1$ m
.

In the vicinity of the asymptote, an unintuitive phenomenon occurs: some of the gas condenses, the liquid obtained has a higher temperature due to the latent energy obtained, the thermal conduction re-equilibrates the temperatures. The gas finally has a greater pressure: the variation in temperature and volume prevail over the diminution in quantity of matter.

See also B.1 for an analytical study of this phenomenon.

3.2.3 Case 3. – Influence of the total height of the system

Initial conditions

We will take $z_0 = 1/i$ meter, for $i \in [1, 10]$.

The other parameters will be $T_0^g = 360$ K, $T_0^l = 380$ K, $P_0 = 1$ bar and $b_0 = 0.05\% \cdot z_0$ (or approximately 50 % in quantity of matter).

Graph

See Figure 3.4.

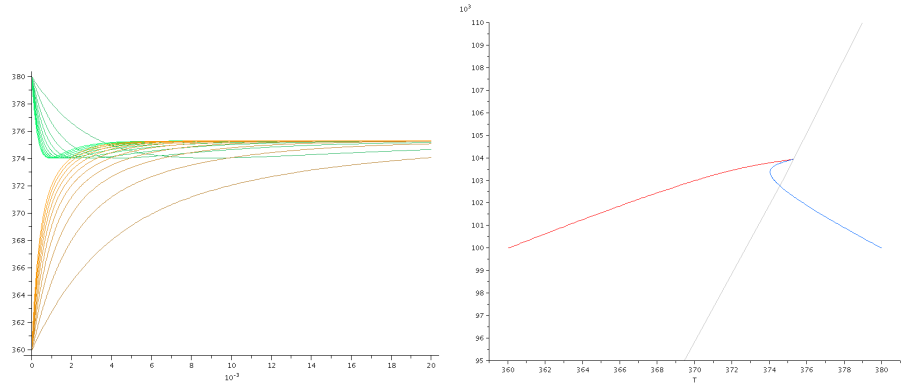

Figure 3.4: *On the left: in orange* the gas temperature (K) and *in green* the temperature of the liquid (K) against time (s).
On the right: pressure diagram (kPa) against temperature (K). *In red* the change in the gas phase, *in blue* the change in the liquid phase. *In grey* the saturation curve $P = P_{\text{sat}}(T)$
Case 3. $z_0 = 1/i$ m ($i \in [1, 10]$), $T_0^g = 360$ K, $T_0^l = 380$ K, $P_0 = 1$ bar and $b_0 = 0.05\% \cdot z_0$

Interpretation

The total height of the system does not influence the path of the system in the diagram $P(T)$ (the paths are superimposed on the graph). Only the timescale of the relaxation of the system is modified. The relaxation is similar to the curve (d) of Case 2.

3.3 Influence of coupling terms

3.3.1 Experiments

3×10 experiments are carried out multiplying the coupling term by an integer factor ranging between 0 and 9 for three sets of initial conditions. The curves resulting from these three experiments are displayed on the same graph in Figures 3.5, 3.6 and 3.7; the indices 0 and 9 enable the different couplings to be located.

The three experiments have the following initial conditions:

1. $P_0^g = 1$ bar, $T_0^g = 370$ K, $T_0^l = 380$ K, $z_0 = 1$ m, $b_0 = 0.01 \cdot z_0$
2. $P_0^g = 1$ bar, $T_0^g = 370$ K, $T_0^l = 380$ K, $z_0 = 1$ m, $b_0 = 0.00001 \cdot z_0$
3. $P_0^g = 1$ bar, $T_0^g = 380$ K, $T_0^l = 370$ K, $z_0 = 1$ m, $b_0 = 0.001 \cdot z_0$

3.3.2 Résultats

See Figures 3.5, 3.6 and 3.7.

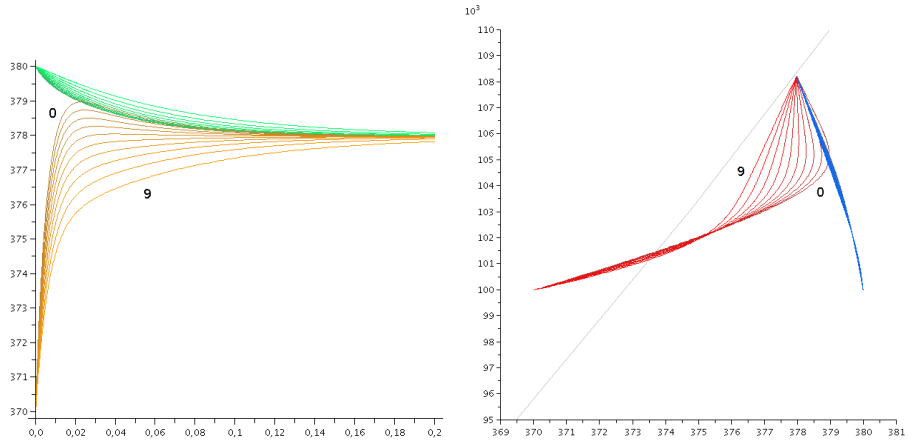

Figure 3.5: *On the left :* temperatures against time. *On the right :* diagram $P(T)$. The legends are the same as in the previous graphs. We have drawn the ten curves here for a multiplication of the coupling coefficients by an index ranging from 0 to 9.

As expected, the terms of the couplings have no impact on the final result. In effect the final state is determined by the resolution of $T_g = T_l$ and $\mu_g = \mu_l$ which do not depend upon transfer coefficients.

In the first experiment, they clearly have an effect of slowing down the relaxation: the curve 0 converges more rapidly than the curve 9. This state is less visible in the two other experiments. It was expected that the coupling would be in opposition to the relaxation due to the negative sign of these coefficients.

Neglecting coupling he comparison of the rate of these first two curves of each graph (curves 0 and 1 – no coupling and normal coupling) seems to justify the possibility of neglecting the coupling terms.

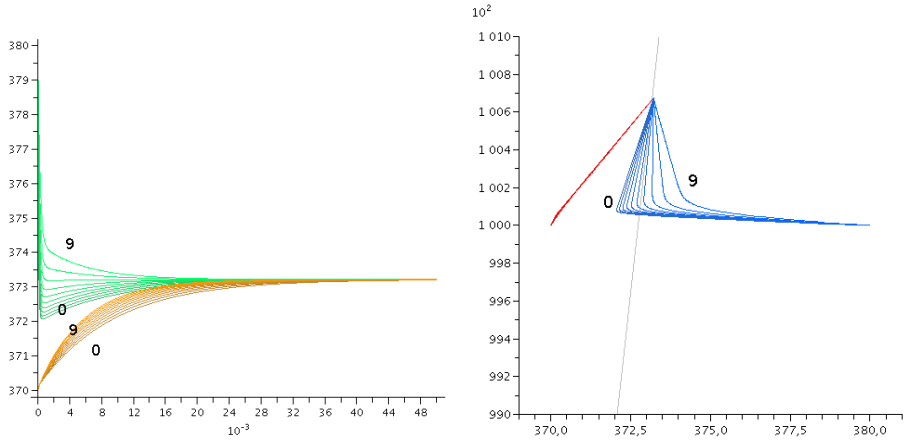

Figure 3.6: Ditto for the second set of initial conditions.

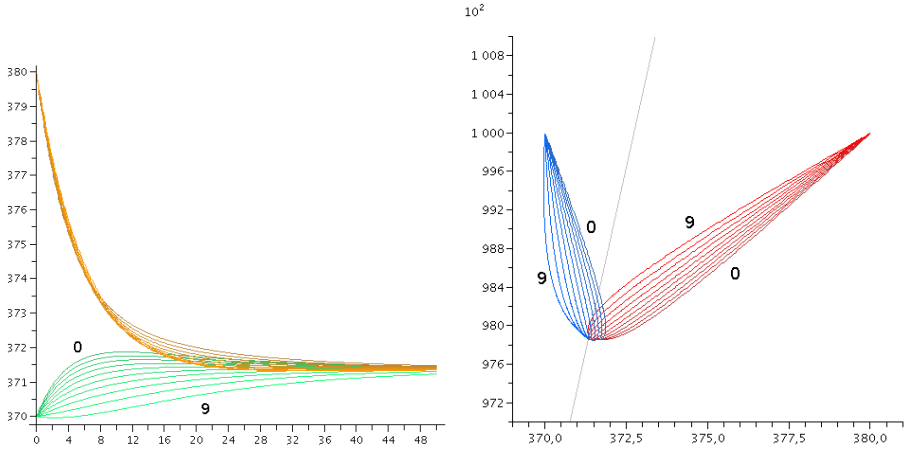

Figure 3.7: Ditto for the third set of initial conditions.

3.4 Other results

3.4.1 Approximation of the thermodynamic force

In the expression of the thermodynamic force (2.17), we have cited the possibility of only retaining the term in logarithm. This hypothesis can be verified numerically.

Figure 3.8 presents the relative values of the different terms for $P_0 = 1$ bar, $T_0^g = 370$ K, $T_0^l = 380$ K, $z_0 = 1$ m and $b_0 = 0.01 \cdot z_0$.

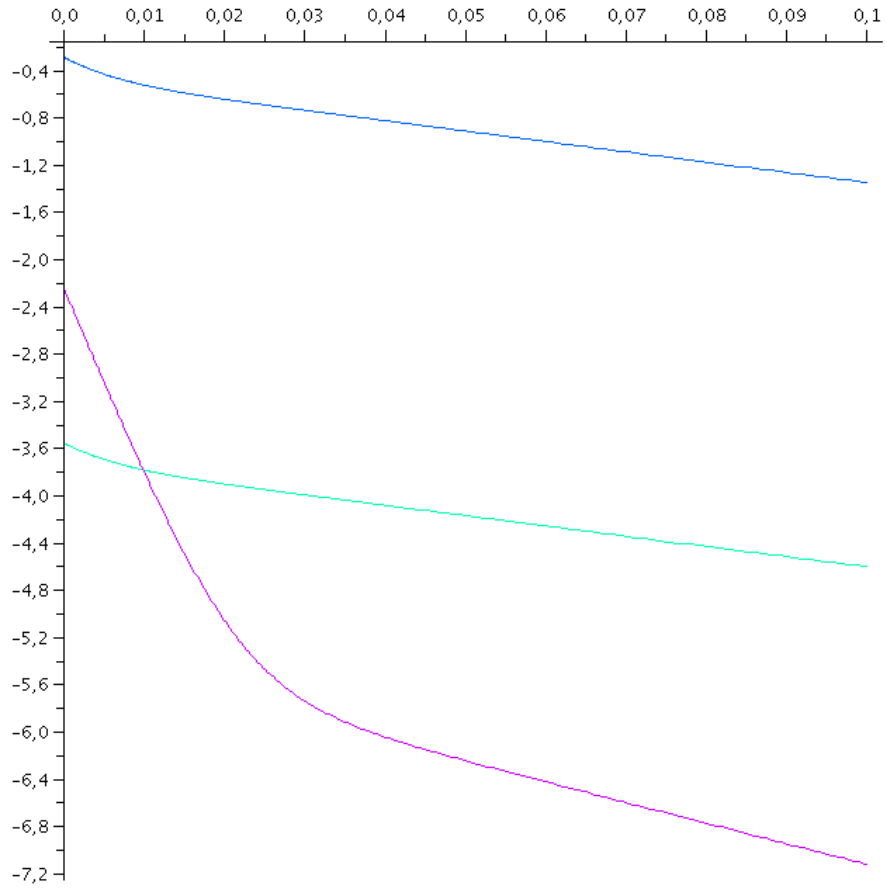

Figure 3.8: Absolute values in a decimal logarithmic scale of the different terms of $(\mu_l(T_l) - \mu_g(T_l))/T_l$ against time (s): the main term $R\ln(P_{\text{sat}}(T_l)/P_g)$ (*in blue*), and the neglected terms $\mathcal{M}/\rho_l T_l(P_l - P_{\text{sat}}(T_l))$ (*in green*) and $\frac{1}{2}\mathcal{C}_g(1 - T_g/T_l)^2$ (*in violet*).

Similar results are observed in all the cases tested in this document. The terms that can be neglected are of two to three orders of magnitude less than the main term.

We should comment that the two terms that can be neglected are often opposite signs and can cancel each other out

3.4.2 Variation in the coefficients of the kinetic theory

The transfer coefficients derived from kinetic theory (presented in the equations (2.23)) are used here for the numerical resolution. The graphs in Figure 3.9 present their variation over time for some of the test cases derived from sections 3.2.1 and 3.2.2.

Many items of information can be deduced from these:

a. The L_{qq} coefficient is the largest but also the one that varies the most over time (up to 120% of its initial value). Conversely, $L_{\mu\mu}$ is the smallest and the one that varies relatively the least

b. The variations are greater for small quantities of gas against liquid. This can be understood in the light of the dependency of the coefficients in the gas parameters.

In conclusion, the hypothesis of constant coefficients over time greatly facilitates calculations but does not always conform to the original model.

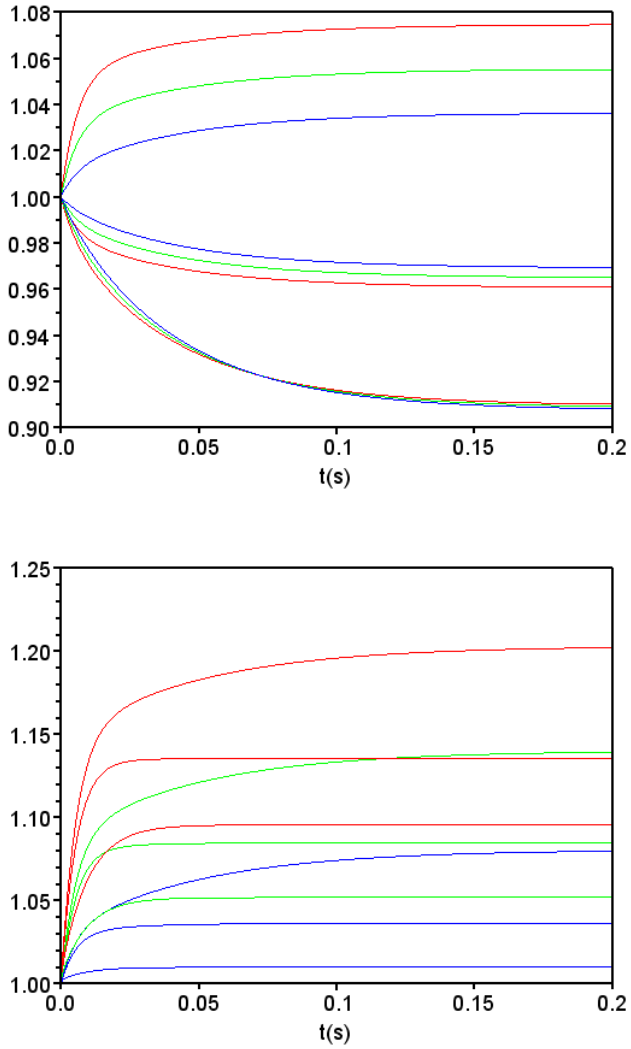

Figure 3.9: Variations of the transfer coefficients over time relatively to their initial value.
In red : L_{qq} ; in green : $L_{q\mu}$; in blue : $L_{\mu\mu}$.

Above: for relaxations derived from Case 1 (from bottom to top):
$P_0^g = 110$ kPa, $T_0^g = 372.5$ K, $z_0 = 1$ m, $T_0^l = 370$ K and $b_0 = 0.01 \cdot z_0$
$P_0^g = 100$ kPa, $T_0^g = 372.5$ K, $z_0 = 1$ m, $T_0^l = 370$ K and $b_0 = 0.01 \cdot z_0$
$P_0^g = 90$ kPa, $T_0^g = 362.5$ K, $z_0 = 1$ m, $T_0^l = 370$ K and $b_0 = 0.01 \cdot z_0$

Below: for relaxations a, c and e derived from Case 2 (the largest variations correspond to a, the smallest to e).

Part II

Mobile piston

Chapter 4

Complete dimensional and dimensionless model

4.1 Description of the system

The system is used as presented in chapter 1. The upper wall of the container is now a mobile piston.

The same set of variables is considered (e, E, n, N, z) ; E and z are no longer constant. The variable $v = \dot{z}$ will be added if we wish to obtain a first order differential equations system.

The external pressure (above the piston) P_u may be considered constant or varying like the pressure in a cavity containing a compressible but non-condensable gas like in the Bagnold model.

4.2 Differential equations

The differential equations system governing the system becomes:

$$\frac{d}{dt}e = \Phi_q(e, E, n, N, z) + \dot{W}_{\text{piston}}(e, E, n, N, z), \tag{4.1a}$$

$$\frac{d}{dt}n = \Phi_\mu(e, E, n, N, z), \tag{4.1b}$$

$$\frac{d}{dt}E = \dot{W}_{\text{piston}}(e, E, n, N, z), \tag{4.1c}$$

$$\frac{d}{dt}N = 0. \tag{4.1d}$$

Equation for the piston movement

The fifth equation of the system is the fundamental relation of the dynamic applied to the piston:

$$\frac{d^2}{dt^2}z = \frac{P_g(e, E, n, N, z) - P_u(z)}{M_{\text{piston}}} \tag{4.1e}$$

where $P_u(z)$ is the pressure above the piston and M_{piston} is the mass of the piston. A new initial condition $v_0 = \dot{z}_0$ will be added to the system (e_0, n_0, E_0, N, z_0).

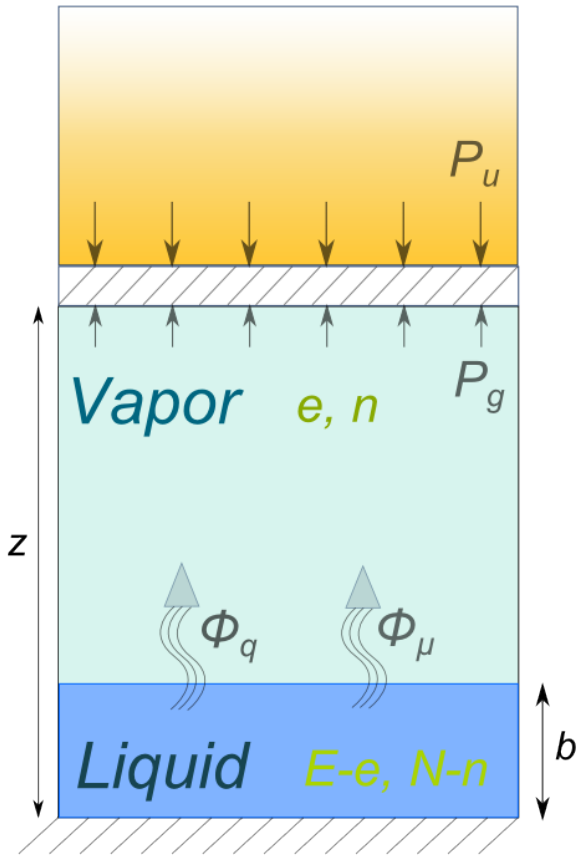

Figure 4.1: Diagram of the system studied

Work exchanged

The work exchanged by the gas with the exterior in the piston movement is

$$\dot{W}_{\text{piston}}(e, E, n, N, z) = -P_g(e, E, n, N, z)\dot{z}. \tag{4.2}$$

Comment The work supplied by the piston is (to the nearest sign) $(P_g - P_u)\,\dot{z}$. This energy is exchanged with the gas under the piston (term $P_g\dot{z}$) and with the gas above the piston (term $P_u\dot{z}$). The system on which we perform an energy analysis is the gas under the piston: the equation (4.2) only contains the term $P_g\dot{z}$.

External pressure

The pressure above the piston may depend on z if the cavity above the piston is of the final volume.

$$P_u(z) = P_{ext}\left(1 + a\left(1 - \frac{z}{z_0}\right)\right)^{-\chi} \qquad \text{where } a = \frac{z_0}{H_{sup}}. \tag{4.3}$$

We have χ which is the gas constant (presumed to be ideal) and H_{sup} which is the height of the cavity above the piston at the initial point in time. For a constant pressure (or in an equivalent manner a cavity of infinite size) we will take $a = 0$.

Fluxes between the phases

Φ_μ and Φ_q are fluxes of matter and energy exchanged between the liquid and vapor phases. The expressions will be those in chapter 2, already applied in chapter 3.

4.3 Dimensionless equations

4.3.1 Prior definitions

Hypotheses

Many hypotheses are posited in order simplify the presentation of the dimensionless equations:

a. In this section, we shall consider the change in the system from a state of initial equilibrium and in the vicinity of this state. In other words $T_{ref} = T_0^g = T_0^l \equiv T_0$ and $P_{ref} = P_{\text{sat}}(T_0) \equiv P_0$.

b. It has been decided that the coupling terms $L_{q\mu} = L_{\mu q} = 0$ will be disregarded. The two other coefficients will be considered as constant.

c. In addition, the inverse difference in temperatures $1/T_1 - 1/T_2$ are approached by a difference in temperature $(T_2 - T_1)/T_0^2$ considering the two temperatures T_1 and T_2 to be in the vicinity of T_0.

d. Finally, we completely disregard the variations in volume caused by the evaporation or condensation of the gas. With a fixed piston, the volume available for the gas will be the same whatever the quantity of matter in liquid form. This level will be recorded as z[1].

In addition, here we use the relation of the vapor pressure given by the Clapeyron relation (1.3b). The reference energies (1.1) are $\mathcal{E}^g_{ref} = 0$ and $\mathcal{E}^l_{ref} = -\mathcal{L}_{\text{vap}}$.

Dimensionless variables

We consider the dimensionless variables $\epsilon,\ \eta,\ \nu,\ \zeta,\ \upsilon$ defined by:

$$e(t) = N_0 \mathcal{L}_{\text{vap}}\, \epsilon(\tau), \tag{4.4a}$$
$$E(t) = N_0 \mathcal{L}_{\text{vap}}\, \eta(\tau), \tag{4.4b}$$
$$n(t) = N_0\, \nu(\tau), \tag{4.4c}$$
$$z(t) = z_0\, \zeta(\tau), \tag{4.4d}$$
$$v(t) = v_0\, \upsilon(\tau), \tag{4.4e}$$
$$\text{where} \quad \tau = \omega t = \frac{v_0}{z_0} t.$$

Dimensionless numbers

The dimensionlessness of the system shows the following magnitudes without dimensions:

$$\kappa_g = \frac{\mathcal{C}_g}{R}, \qquad \kappa_l = \frac{\mathcal{C}_l}{R}, \tag{4.5a}$$
$$\Lambda = \frac{\mathcal{L}_{\text{vap}}}{RT_0}, \qquad \nu_0 = \frac{n_0}{N_0}. \tag{4.5b}$$

We also find the dimensionless number S (the *impact number*) as in the Bagnold model without phase change.

$$S = \frac{M_{\text{piston}} v_0^2}{P_0 z_0} \tag{4.5c}$$

Finally, we note the appearance of two numbers without dimensions, which are comparable to characteristic frequencies for the transfer of energy and matter:

$$\Omega_e = \frac{L_{qq}}{N_0 T_0^2 C_l} \frac{1}{\omega} = \frac{\nu_0}{\kappa_l} L_{qq} \frac{1}{P_0 z_0 T_0} \frac{1}{\omega}, \tag{4.5d}$$

$$\Omega_n = \frac{L_{\mu\mu} R}{N_0} \frac{1}{\omega} = L_{\mu\mu} \frac{R^2 T_0}{P_0 z_0} \frac{1}{\omega}. \tag{4.5e}$$

[1] In the previous sections, the volume of gas was $z - b$. Now that the variations of b are disregarded, the volume of gas is simply recorded as z.

Dimensionless expressions of thermodynamic magnitudes of the system

The usual thermodynamic magnitudes of the system have the following expression:

$$T_g = T_0 \left(1 + \frac{\Lambda}{\kappa_g}\frac{\epsilon}{\nu}\right), \tag{4.6a}$$

$$T_l = T_0 \left(1 + \frac{\Lambda}{\kappa_l}\left(\frac{\eta - \epsilon}{1-\nu} + 1\right)\right), \tag{4.6b}$$

$$P_g = \frac{P_0}{\nu_0}\left(\frac{\nu + \epsilon\frac{\Lambda}{\kappa_g}}{\zeta}\right). \tag{4.6c}$$

4.3.2 Dimensionless differential equations

The differential equations of the system are as follows:

$$\frac{d\epsilon}{d\tau} = \Omega_e \left(\frac{\eta - \epsilon}{1-\nu} + 1 - \frac{\epsilon}{\nu}\frac{\kappa_l}{\kappa_g}\right) + \left(\frac{\epsilon}{\nu}\left(1 + \frac{1}{\kappa_g}\right) + \frac{1}{\Lambda}\right)\frac{d\nu}{d\tau} + \frac{d\eta}{d\tau}, \tag{4.7a}$$

$$\frac{d\eta}{d\tau} = -\frac{1}{\Lambda}\frac{\nu + \frac{\Lambda}{\kappa_g}\epsilon}{\zeta}\upsilon, \tag{4.7b}$$

$$\frac{d\nu}{d\tau} = \Omega_n \left[\ln\left(\frac{\nu_0\zeta}{\nu + \frac{\Lambda}{\kappa_g}\epsilon}\right) + \frac{\Lambda^2}{\kappa_l}\left(\frac{\eta - \epsilon}{1-\nu} + 1\right)\right], \tag{4.7c}$$

$$\frac{d\zeta}{d\tau} = \upsilon, \tag{4.7d}$$

$$\frac{d\upsilon}{d\tau} = \frac{1}{S}\left(\frac{\nu + \frac{\Lambda}{\kappa_g}\epsilon}{\nu_0\zeta} - \frac{P_u}{P_0}\right). \tag{4.7e}$$

Comment The preponderance of the dimensionless number Λ is explained more by the choice of $N_0\mathcal{L}_{\text{vap}}$ as reference in (4.4) than by the fact that we are studying phase change.

Initial conditions

The initial conditions associated with this problem are

$$\epsilon(0) = 0, \tag{4.8a}$$

$$\eta(0) = \nu_0 - 1, \tag{4.8b}$$

$$\nu(0) = \nu_0, \tag{4.8c}$$

$$\zeta(0) = 1, \tag{4.8d}$$

$$\upsilon(0) = \pm 1. \tag{4.8e}$$

4.4 Back to the Bagnold model

With the same formalism, the Bagnold model can be re-written without phase change (or heat exchanges between the phases).

Dimensioned equations

By positing $\Phi_q = 0$ and $\Phi_\mu = 0$:

$$\frac{d}{dt}e = \dot{W}_{\text{piston}}(e, n, z), \tag{4.9a}$$
$$\frac{d}{dt}n = 0, \tag{4.9b}$$
$$\frac{d}{dt}E = \dot{W}_{\text{piston}}(e, n, z), \tag{4.9c}$$
$$\frac{d}{dt}N = 0, \tag{4.9d}$$
$$\frac{d^2}{dt^2}z = \frac{P_g(e, n, z) - P_u(z)}{M_{\text{piston}}}. \tag{4.9e}$$

It will be noted that that one can also study (as in 5.3.1) the intermediate case of a liquid-vapor system without phase change but with heat exchanges between the phases by positing only $\Phi_\mu = 0$.

The case of a system without heat exchange but with phase change would be of little relevance in our model (the exchanged matter will carry energy).

Dimensionless equations

By positing $\Omega_e = 0$ and $\Omega_n = 0$:

$$\frac{d\epsilon}{d\tau} = \frac{d\eta}{d\tau}, \tag{4.10a}$$
$$\frac{d\eta}{d\tau} = -\frac{1}{\Lambda}\,\frac{\nu + \frac{\Lambda}{\kappa_g}\epsilon}{\zeta}\upsilon, \tag{4.10b}$$
$$\frac{d\nu}{d\tau} = 0, \tag{4.10c}$$
$$\frac{d\zeta}{d\tau} = \upsilon, \tag{4.10d}$$
$$\frac{d\upsilon}{d\tau} = \frac{1}{S}\left(\frac{\nu + \frac{\Lambda}{\kappa_g}\epsilon}{\nu_0\zeta} - \frac{P_u}{P_0}\right). \tag{4.10e}$$

The intervention of magnitudes ν_0 and Λ is a consequence of the choice of $N_0\mathcal{L}_{\text{vap}}$ as dimensionlessness coefficient in the energy magnitudes in (4.4) (which is scarcely relevant in the context of the Bagnold model without phase change).

It is to this system that we shall refer subsequently as the dimensionless Bagnold model.

Chapter 5

Numerical resolutions

5.1 General

Implementation

The results presented below are the resolution of the dimensionless equations (4.7) using Matlab. The numerical values given in table 3.1 are used.

Structure of the chapter

Two phenomena can be observed:

a. an effect due solely to heat exchanges (presented and interpreted in 5.3.1)

b. an effect due to phase change.

These two effects (at least) are superimposed in the results in 5.2, 5.3.2, and in 5.3.3.

5.2 Results: functions of time

Results

Figures 5.1 and 5.2 present two examples of typical results. In particular they illustrate the influence of ν_0 in the dynamic of the system..

Comments

General presentation The results are more or less amortized oscillations. Their period is fairly close to that of the Bagnold model.

Role of ν_0 According to the initial conditions chosen, the amplitude of the oscillations is more or less amortized. The determining parameter seems to be ν_0: for large values of ν_0 the oscillations are slightly amortized (figure 5.1); for small values of ν_0 the oscillations are significantly amortized (figure 5.2).

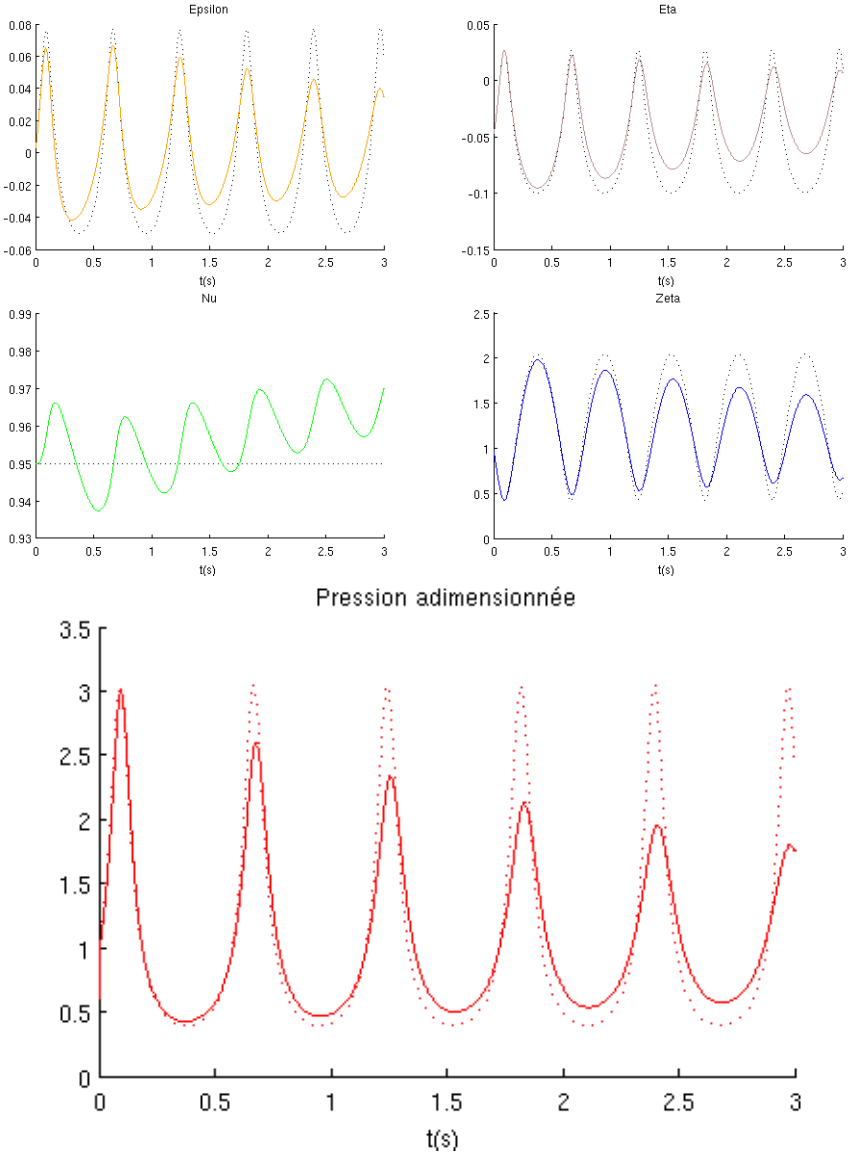

Figure 5.1: Results of the numerical resolution for the following parameters: $\nu_0 = 0.95$, $T_0 = 373$ K, $S = 0.8$, $\omega = 8.9$ s^{-1}, $L_{qq} = 10^9$, $L_{\mu\mu} = 1$.

Top left : ϵ, gas energy;
top right : η, total energy;
centre left : ν, quantity of matter;
centre right : ζ, piston height;
bottom : P/P_0, pressure.
The curves in dotted lines correspond to the Bagnold model (without phase change) for the same initial conditions.

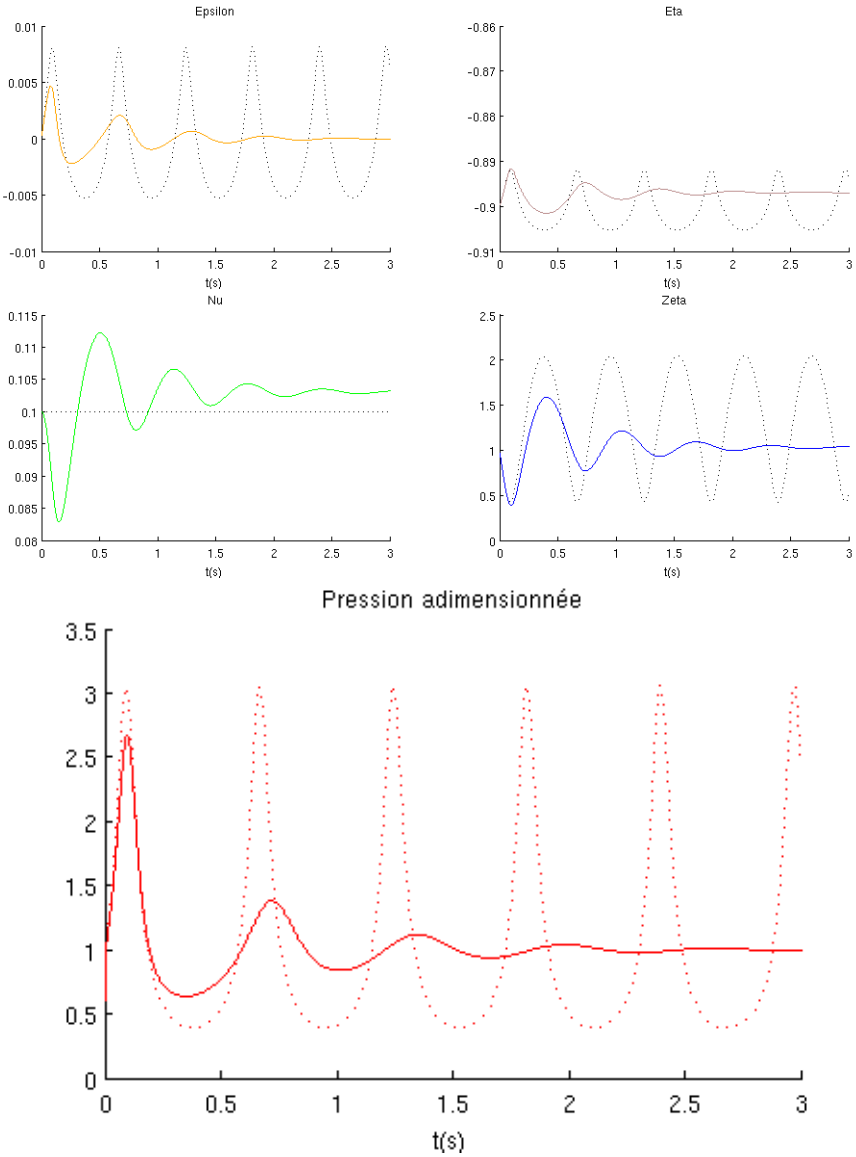

Figure 5.2: Results of the numerical resolution for the following parameters: $\nu_0 = 0.1$, $T_0 = 373$ K, $S = 0.8$, $\omega = 8.9$ s^{-1}, $L_{qq} = 10^9$, $L_{\mu\mu} = 1$.

Top left : ϵ, gas energy;
top right : η, total energy;
centre left : ν, quantity of matter;
centre right : ζ, piston height;
bottom : P/P_0, pressure.
The curves in dotted lines correspond to the Bagnold model (without phase change) for the same initial conditions.

Role of S The role of the impact number S is the same as in the Bagnold model: a larger value for S entails more marked and higher peaks of pressures

We shall also refer to section 5.3.2 for further detail on the influence of S and ν_0.

5.3 Results: functions of the parameters

Rather than dealing with the entire temporal signal, in the following paragraphs we shall study the variations in two magnitudes:

- the height of the first pressure peak (to be compared with the height of the oscillations in the Bagnold model);
- the difference in height between the first two pressure peaks (to judge the amortization of the oscillations).

5.3.1 Heat exchanges alone

Results

Figure 5.3 presents the pressure for different values of Ω_e. It has been obtained by artificially varying L_{qq}, with the other parameters remaining fixed.

Comments and interpretation

a. $\Omega_e \ll 1$: The heat transfer is too slow to have an influence on the oscillations. The peaks of pressure are identical to those of the Bagnold model.

b. $\Omega_e \gg 1$: The oscillations are sinusoidal, but it will be noted that there is a slight variance from the Bagnold model. Numerically, it is noted that this variance is all the greater when there is a large quantity of liquid (without exceeding $0.1P_0$ for $S = 0.5$). In addition, one may note a diminution in amplitude of the variations in ϵ (not plotted here).

   One may interpret these observations due to the "energy storage" role played by the liquid. The result obtained is in fact similar to that of the Bagnold model for a greater thermal capacity of the gas:

$$n_g \mathcal{C}_g^{\text{eq}} = n_l \mathcal{C}_l + n_g \mathcal{C}_g \tag{5.1}$$

c. $\Omega_e \sim 1$: A phenomenon of amortization of oscillations is observed: the following paragraph attempts an interpretation of this phenomenon.

Interpretation of the resonance

We shall here attempt a physical interpretation of the amortization phenomenon by comparing our system to a thermal machine receiving work. One may take the example of the Carnot cycle.

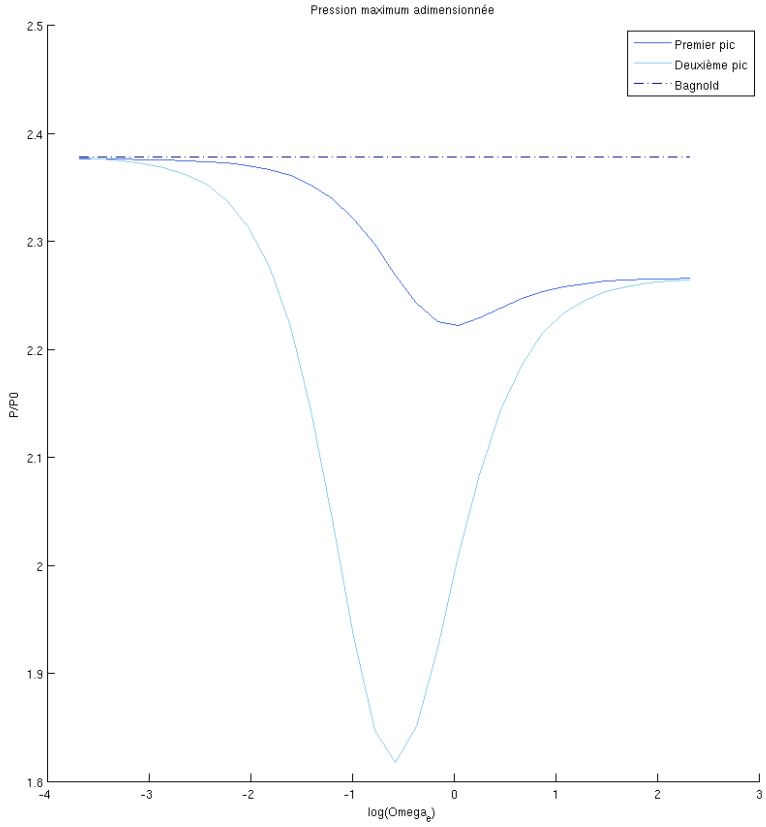

Figure 5.3: Dimensionless pressure as a function of $\log(\Omega_e)$ in the absence of exchanges of matter.
$\Omega_n = 0$, $S = 0.5$, $\nu_0 = 0.5$, $T_0 = 373$ K
In dark blue: first pressure peak; *in light blue*: second pressure peak; *dotted*: Bagnold model.

Carnot cycle (receptor) This type of cycle is divided into four phases:

1. adiabatic compression;
2. heat exchange with a *cold source* ;
3. adiabatic relaxation;
4. heat exchange with a *hot source*.

It converts the work of the piston into heat energy dissipated into the thermostats. The greater the variance of temperature between the sources, the greater the efficiency of the cycle.

In our system The liquid (whose temperature oscillates) alternately plays the role of a hot and cold source. As the characteristic energy exchange time between the phases is not null, the liquid temperature is "delayed" in respect of the gas temperature

- The temperature of the liquid is less than that of the gas in the compressions phase (stages 1 and 2 above).
- The temperature of the liquid is greater than that of the gas in the decompression phase (stages 3 and 4 above).

Our system therefore behaves like a thermal machine (whose efficiency is very low however). For a well-chosen heat exchange frequency, the temperature of the liquid will be minimal at the point in time when it is a "cold source" and maximal at the point in time when it is a "hot source". Thus, the efficiency of the thermal machine increases and an amortization can be observed on the curve 5.3.

5.3.2 Influence of S and ν_0

Pressure

Figure 5.4 presents the results obtained for different values of S and ν_0.

Extreme cases in ν_0 Figures 5.1 and 5.2 correspond to the right and left extremities of the graph 5.4.

For values of ν_0 of less than 0.1, we encounter cases where all the gas passes into liquid form and the piston touches the bottom of the tank. Similarly, for values of ν_0 greater than 0.9, we encounter cases where all the liquid evaporates with the first raising of the piston.

Raising time

The figure 5.5 presents the raising time (point in time when the first pressure peak is reached) as a function of S.

The phase change has relatively little impact on this value, and this is regardless of the selected value of ν_0.

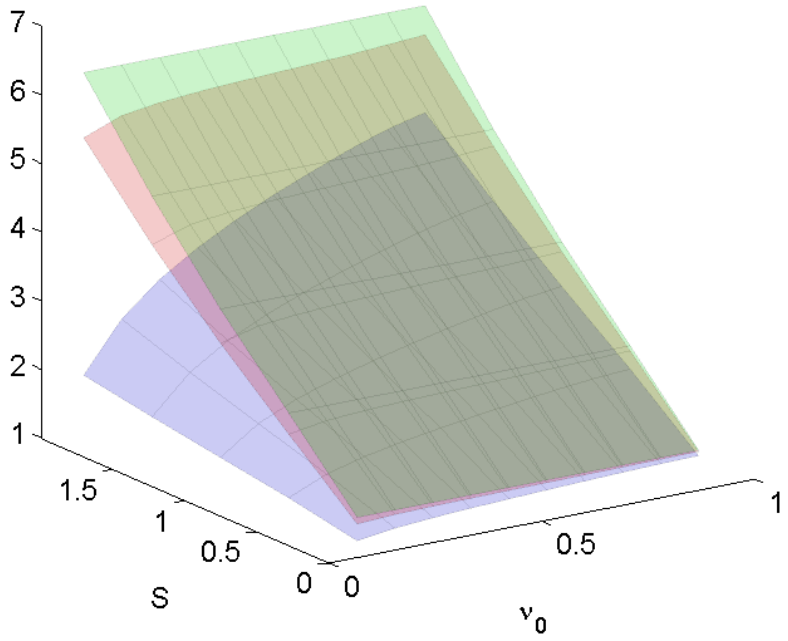

Figure 5.4: Maximum dimensionless pressure as a function of the two parameters ν_0 (horizontally) and S (in depth).
$T_0 = 373$ K, $L_{qq} = 10^9$, $L_{\mu\mu} = 1$
ω is calculated from $M_{\text{piston}} = 1000$ kg, $z_0 = 1$ m and from S
In green: Bagnold model;
in red: first pressure peak;
in blue: second pressure peak.

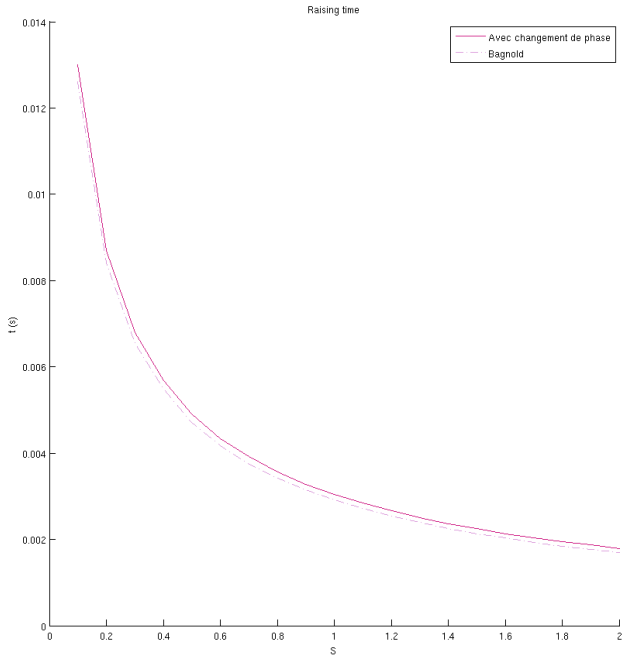

Figure 5.5: Raising time (point in time when the first pressure peak is reached) as a function of S.
$\nu_0 = 0.95$, $T_0 = 373$ K, $L_{qq} = 10^9$, $L_{\mu\mu} = 1$
ω is calculated from $M_{\text{piston}} = 1000$ kg, $z_0 = 1$ m and from S
Dotted line: Bagnold model; *solid line:* phase change model.

5.3.3 Influence of L_{qq} and $L_{\mu\mu}$

Figure 5.6 presents the pressure for different values of Ω_e and Ω_n. It is obtained by artificially varying L_{qq} and $L_{\mu\mu}$, with the other parameters remaining fixed

We note two resonance phenomena:

- a thermal resonance in Ω_e, already studied in 5.3.1 ;
- a resonance of greater amplitude in Ω_n.

One can refer to the interpretations in section 5.3.1 for an attempt at understanding this phenomenon.

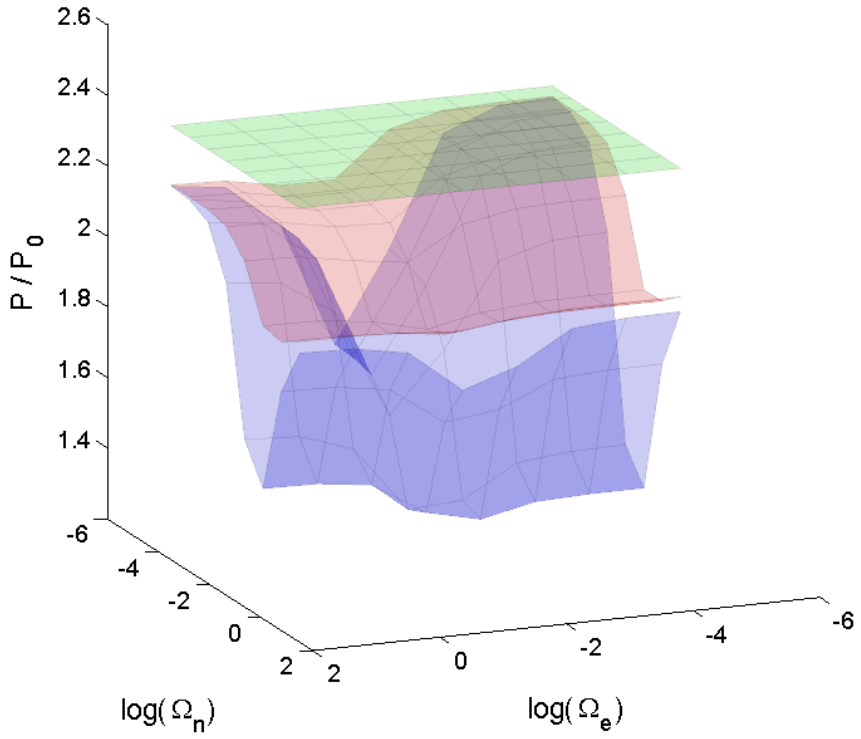

Figure 5.6: Maximal pressure as a function of $\log(\Omega_e)$ and $\log(\Omega_n)$
$T_0 = 373$ K, $\omega = 7.07$ s^{-1}, $S = 0.5$, $\nu_0 = 0.1$
In green: Bagnold model;
in red: first pressure peak;
in blue: second pressure peak.

Chapter 6

Conclusion

6.1 Conclusion

We have shown in the course of this work the effect of a phase change in the Bagnold model. The attenuation of oscillations in this model could explain the previous experimental results.

It will be remembered however, that many hypotheses have been proposed in the course of this work. Namely:

a. Ideal gas, constant thermal capacities, constant mass density of liquid;

b. Homogeneous temperatures in the gas and in the liquid;

c. Linear forces/fluxes equations with L_{qq} and $L_{\mu\mu}$ coefficients whose values remain to be determined;

d. The use in transitory regime of equations developed for the permanent regime.

The validity interval of these previous approximations is *a priori* difficult to determine.

The validity of this model in the context of an industrial application remains therefore to be verified.

6.2 Proposed improvements

Amongst the many improvements that it is possible to apply to the model to make it closer to reality, the following three are selected here, in order of importance.

Temperature gradient

In the previous results we saw the importance of the question of energy storage, of its transport and of its exchange. For example the increase in quantity of liquid leads to an increase in the overall thermal capacity of the system and directly influences the results.

For greater pertinence of the results, it would therefore be necessary to introduce a temperature gradient along the z axis.

It should be noted that the transfer equations uses in this document can be adapted to the problem in one dimension.

Extreme limit cases: first drop, last bubble

As it is, the model does not enable resolution of the extreme limit cases of liquid-vapor equilibrium, such as, for example, the appearance of a drop of liquid in a purely gaseous system. A more precise study of the phase change phenomena is required here.

Added to the idea of the temperature gradient, this phenomenon may considerably enrich the model. In effect, it would enable phase changes to be taken into account outside the interface. If one considers for example an elementary volume of liquid far from the interface, it may be envisaged that a part of this volume vaporises (under the effect of a temperature that is too high, for example), with the gas then escaping to the surface.

More heat exchanges

Still with the same idea (how does the energy travel in the system?), one can also consider the possibility of adding more heat exchanges with exterior of my system.

In particular, one may envisage that:

- the piston is not adiabatic and exchanges heat energy with the system;
- the piston exchanges matter through phase change with the gas and is not of consistent mass.

While the first effect may play an important role in the evolution of the system, the second effect will a priori be negligible: the order of magnitude of the mass of the piston being greater than that of the mass of matter changing phase during an oscillation.

Similarly, it may be useful to study in more detail the role of heat leakages on the walls and base of the tank.

Part III

Appendix and bibliography

Appendix A

Chronology and bibliography of the models

In this chapter, we shall present the different models found in the literature for liquid-vapour exchanges.

Bond [Bon04] as well as Badam et al. [BKDD07] present as an introduction to their work an overview of the different models that have been proposed.

A.1 Hertz and Knudsen

The first work in this field is that of Hertz ($\sim$ 1885) and subsequently Knudsen ($\sim$ 1915). Using the basis of the kinetic theory of gasses, they deduce the following relation:

$$\Phi_\mu = \sqrt{\frac{\mathcal{M}}{2\pi R}}\left(\sigma_{ev}\frac{P_{\text{sat}}(T_l)}{\sqrt{T_l}} - \sigma_{con}\frac{P_g}{\sqrt{T_g}}\right) \quad (\text{in } kg\cdot m^{-2}\cdot s^{-1}) \tag{A.1}$$

where σ_{ev} and σ_{con} are the (empirical) evaporation and condensation coefficients, added a posteriori to the theory to make it conform the experiment. Most of the subsequent work, such as that of Schrage ($\sim$ 1950), was based on this equation.

One can find details on the demonstration of this formula for example in [Bon04].

Coefficients

These coefficients could be roughly interpreted as the probability of phase change for a molecule in contact with the liquid-vapour interface. They therefore have a value of between 0 and 1 and are often considered to be equal (they should be so at equilibrium). They have been (are being) studied in detail, without a definitive value or expressing being derived from them

Eames et al. [EMS97] as well as Marek and Straub [MS01] synthesise several of these experimental measurements.

Research on this subject is still very active and many papers explore the possible expressions for these coefficients (for example in [Bon04], resumed in [BS04])

Comment The relation (A.1) could be in contradiction with the principles of conservation of energy and quantity of movement [BKDD07, p.285]

A.2 Ward and Fang (Toronto, Canada)

Experimental results

At the end of 1990, the experimental mechanism of Fang and Ward [FW99b], which was more precise that the previous studies, showed a jump in temperature in the vicinity of the surface between the two phases. This jump is 10 to 20 times greater than that which was expected by existing models [BKDD07, p.285].

This work, which provided a large number of experimental measurements, rekindled interest in the subject.

SRT

Ward and Fang themselves propose a new model based on the *Statistical Rate Theory* (SRT) [WF99, FW99a, War02]. The expression of the flux of matter is as follows:

$$\Phi_\mu = 2K_e \sinh\left(\frac{\Delta s_{lg}}{k}\right) \qquad \Delta s_{lg} = \frac{\mu_l}{T_l} - \frac{\mu_g}{T_g} + \mathcal{H}^g\left(\frac{1}{T_g} - \frac{1}{T_l}\right) \tag{A.2}$$

where k is the Boltzmann constant and K_e is:

$$K_e = \frac{P_{sat}(T_l)}{\sqrt{2\pi m k T_l}} \exp\left(\frac{v^l}{kT^l}\left(P^l_{eq} - P_{sat}(T_l)\right)\right) \quad (\text{in } m^{-2}\cdot s^{-1}) \tag{A.3}$$

where m is the mass of a particle, P^l_{eq} is the pressure of the liquid at equilibrium and v^l is the volume mass of the liquid phase.

They also present an expression of the difference between chemical potentials as a function of the pressures, temperatures and microscopic characteristics of the molecules (functions of the partition of vibrations).

This formulation presents the advantage of not leaving any free parameter. However it does not provide an expression for a flux of heat, which is disregarded in its demonstration.

A.3 Bedeaux and Kjelstrup (Trondheim, Norway)

Dick Bedeaux, Signe Kjelstrup and their collaborators worked in depth on the modelling of transfers of mass, energy and charges through interfaces, and did so by applying the principles of *Non-Equilibrium Thermodynamics* (NET) – also sometimes referred to as the *Thermodynamics of Irreversible Processes* (TIP).

A.3.1 General expressions of NET

We find expressions of this model in [BK99], [BK05], [KB08], as well as in more or less partial form in other documents cited in this section.

[BK05] presents a general theoretical approach to exchanges of mass, charges and energy through an interface. The same equations are developed in [KB08] and applied more specifically in the case of the liquid-vapour phase change.

The presentation of the equations is as follows (see sections 2.3 and 2.4 for further detail):

$$\Phi_q = L_{qq}\left(\frac{1}{T_g} - \frac{1}{T_l}\right) + L_{q\mu}\left(\frac{\mu_l}{T_l} - \frac{\mu_g}{T_g}\right) \tag{A.4a}$$

$$\Phi_\mu = L_{\mu q}\left(\frac{1}{T_g} - \frac{1}{T_l}\right) + L_{\mu\mu}\left(\frac{\mu_l}{T_l} - \frac{\mu_g}{T_g}\right) \tag{A.4b}$$

The coefficients L_{ij} (free parameters from the theory) can be calculated theoretically from the kinetic theory of gasses (see equations 2.23), using the *Van der Waals square gradient model* [JB04] or using other experimental or numerical methods. These are studied in more detail in section 2.6.

The expression of the difference in chemical potentials is developed in 2.4.

A.3.2 Experimental tests

In [BK99], the results are compared with the water experiments of Ward and Fang [FW99b]. The theoretical results seem to disagree with the experimental results. It has been commented *a posteriori* that certain data collected were incomplete [KB08, p.8].

Badam et al. [BKDD07] have also compared this model with their experimental results on the evaporation of water. The general form of the equations from NET accords well with the experimental results, but the numerical value of the coefficients still seems very approximate

A.3.3 Numerical simulations at molecular level

Given the small amount of experimental data available, the coefficients were compared to several numerical models of interactions at the molecular level. The following paragraphs review some of the articles linked to this question.

NEMD Røsjorde et al. [RFB+00, RKBH01] numerically simulate the phase change using *Nonequilibrium Molecular Dynamic* (NEMD). The system is made up of Argon atoms interacting through a *Lennard-Jones spline potential*.

The results show in particular that the hypothesis of local equilibrium is respected (see 2.1) even for significant temperature gradients and verify the existence of a linear dependency between the fluxes and forces in accordance with NET. The transfer coefficients measured are compatible with the expressions given by the kinetic theory between the triple point and the middle of the saturation curve

Xu et al. [XKB+06] extend this work and confirm these results. They also verify the validity of the relations of reciprocity of Onsager in the context of this problem.

Ge et al. [GKB+07] continue the numerical modelling by using an interaction with a longer range between the particles (*long-range Lennard-Jones spline particles*). The hypothesis of local equilibrium is still verified but a variance is noted with the values of the coefficients of the kinetic theory (even for particles of the Argon type).

Integral relations In [JB06] and [GBSK07], the links are presented between the local transfer coefficients (conductivities - 1D) and the overall coefficients (conductances - 0D). The overall coefficients can be expressed from a single local coefficient which is a function of space

Simon et al. [SBK+06] verify these relations in their simulations, indirectly validating the results from NET. They also carry out tests on a non-monatomic gas (molecules of n-octane) and give values of transfer coefficients for this gas.

A.3.4 Multiple-components

Many other texts deal with the phase change of a mixture of several components. One may cite for example [KK03] which studies the distillation of ethanol and water through NET with coefficients derived from the kinetics of gases. Their results correspond, within margins of error, to the data of an experimental apparatus.

In [ORK02] we find a simulation experiment with NEMD of the phase change of a mixture of two components.

Many other works on the subject are not cited here.

A.4 Synthesis

A.4.1 Links between the models

Despite their obvious differences, the three formulations are linked:

From SRT to NET In the SRT equation (A.2), the approximation $\sinh(x) \approx x$ and the Gibbs-Helmholtz relation (equation (2.10)) enable us to obtain a formulation similar to that from NET without coupling terms. This absence of couplings is easily explained by the fact that SRT does not model heat exchanges between the phases and cannot therefore include the coupling between the two types of exchanges. This reasoning enables us to propose K_e from SRT as the coefficient $L_{\mu\mu}$ for NET.

From NET to Hertz-Knudsen It can also be shown [BKDD07, Bon04] that a development of NET without coupling (or of linearised SRT) in the vicinity of the equilibrium gives us the equation (A.1) from Hertz-Knudsen with condensation and evaporation coefficients equal to 1.

A.4.2 Conclusion

Having reviewed the existing models, Bond [Bon04] concludes that they may all prove relevant for modelling this problem. Badam et al [BKDD07] seems to give more credit to the models based on NET than to the others.

We have chosen to work mainly on the model of non-equilibrium thermodynamics (NET). Amongst the arguments that favour this model are:

- The conservation of energy was one of the objectives of the project: the model ensures for us that the two first principles of thermodynamics are respected.

- The model is complete and does not disregard heat transfers as SRT does.
- The difficult question of the value of the phenomenological coefficients is no more problematic than that of the evaporation and condensation coefficients in the relations derived from Hertz-Knudsen.
- Even though the model is still less mature than that of Hertz-Knudsen, it has been the subject of numerous, more in-depth and validation studies and continues even now to be studied.
- The principles of NET are adaptable to 1D modelling (or higher) of the same problem.

Appendix B

Other comments

B.1 Relation between dP and dn

Let us consider a liquid-vapor system similar to that which is described in chapter 1, in other words in a closed adiabatic vessel of fixed volume.

In order to be able formally to calculate the following result, an additional hypothesis will be posited: the liquid and vapor are permanently in heat equilibrium, and their common temperature is scored at T.

The differentiation of the ideal gas law $PV = nRT$ gives:

$$\frac{dP}{dt} = R\left(\frac{T}{V}\frac{dn}{dt} + \frac{n}{V}\frac{dT}{dt} - \frac{nT}{V^2}\frac{dV}{dt}\right) \tag{B.1}$$

For an insulated vessel, the overall conservation of energy gives:

$$\big(n\mathcal{C}_g + (N-n)\mathcal{C}_l\big)\frac{dT}{dt} = -\mathcal{L}_{\text{vap}}\frac{dn}{dt} \tag{B.2}$$

or, in other words, the phase change of a certain quantity of matter leads to the consumption/recovery of a certain latent vaporisation heat which will influence the temperature of the entire system.

In addition, if one supposes the constant mass density of the liquid:

$$\frac{dV}{dt} = \frac{\mathcal{M}}{\rho_l}\frac{dn}{dt} \tag{B.3}$$

By replacing $\frac{dT}{dt}$ and $\frac{dV}{dt}$ in (B.1), we get:

$$\frac{dP}{dt} = \frac{R}{V}\left(T - \frac{n\mathcal{L}_{\text{vap}}}{(n\mathcal{C}_g + (N-n)\mathcal{C}_l)} - \frac{nT\mathcal{M}}{V\rho_l}\right)\frac{dn}{dt} \tag{B.4}$$

or also

$$\frac{dP}{dt} = \frac{R}{V}\left(T\left(1 - \frac{\rho_g}{\rho_l}\right) - \frac{\mathcal{L}_{\text{vap}}}{\mathcal{C}_g + \frac{N-n}{n}\mathcal{C}_l}\right)\frac{dn}{dt} \tag{B.5}$$

Under normal conditions, $\rho_g \ll \rho_l$, from which, finally:

$$\frac{dP}{dt} = \frac{R}{V}\left(T - \frac{\mathcal{L}_{\text{vap}}}{\mathcal{C}_g + \left(\frac{N}{n} - 1\right)\mathcal{C}_l}\right)\frac{dn}{dt} \tag{B.6}$$

The quantity in brackets is cancelled for:

$$\frac{n}{N} = \nu_c := \frac{\mathcal{C}_l}{\mathcal{C}_l - \mathcal{C}_g + \frac{\mathcal{L}_{\text{vap}}}{T}} \tag{B.7}$$

For a ratio of quantities of matter lower than ν_c, dP is of the same sign as dn: vaporisation is required to increase the pressure of the gas.

For a ratio of quantities of matter greater than ν_c, dP is of an opposite sign to dn: condensation is required to increase the pressure of the gas.

For water at 300 K, $\nu_c \sim 0,5$.

This result is not very intuitive. The notion of phase change is generally studied at constant pressure and/or temperature and we do not really have an intuitive notion of what a phase change would be like in a completely insulated vessel.

B.2 Liquid surface tension

The liquid surface tension was disregarded in the previous sections of this document. It is nonetheless very present in many of the documents in the bibliography (particularly the numerical simulation studies cited in section A.3.3). This section briefly presents some aspects of this order of magnitude.

B.2.1 Succinct presentation

The surface tension is a surface energy present at the liquid-vapour interface. It is responsible for different phenomena, including the spherical form of bubbles and drops or the fact that certain bodies that are more dense than water can remain held on the surface.

It is dependent on the temperature of the surface (and the chemical species under consideration).

It is expressed in $\mathrm{N} \cdot \mathrm{m}^{-1}$.

Order of magnitude $\gamma \simeq 60\,\mathrm{mN} \cdot \mathrm{m}^{-1}$ for water at 100 °C.

B.2.2 Liquid pressure

The surface tension has the consequence of a difference in pressure between the liquid and the gas on the surface.

$$P_l = P_g + \frac{2\gamma}{r} \tag{B.8}$$

where γ is the surface tension and r is the curve radius [BK99].

It is noted that taking a null surface tension ($\gamma = 0$) or a flat surface ($r = \infty$) is equivalent.

For a curve in the order of the centimetre, the difference in pressure is of the order of a dozen pascals. This can be neglected in our study.

B.2.3 Kelvin's equation

In the case of non-flat surfaces, the vapour pressure in the vicinity of the surface may be different to the usual pressure. Kelvin's equation links the surface tension and the radius of the curvature at vapour equilibrium pressure. [BGK03, section 2.5]

$$\ln\left(\frac{P_{\text{sat}}^{\text{courb}}}{P_{\text{sat}}}\right) = \frac{2\gamma\mathcal{M}}{\rho_g RTr} \tag{B.9}$$

where γ is the liquid surface tension and r is the radius of the curvature of the surface.

The pressure of vapour around droplets is higher than on a flat surface (positive curvature). Conversely, it is lower within an air bubble (negative curvature).

$2\gamma\mathcal{M}/\rho_g RT$ is of the order of a nanometre for water at usual values of ρ and T. The change in vapour pressure would be negligible for curvature radii greater than a micrometre.

Bibliography

[Bal03] Roger Balian. Introduction à la thermodynamique hors équilibre, 2003. http://e2phy.in2p3.fr/2003/actesBalian.pdf.

[BGK03] H.J. Butt, K. Graf, and M. Kappl. *Physics and chemistry of interfaces*. Physics textbook. Wiley-VCH, 2003.

[BK99] D. Bedeaux and S. Kjelstrup. Transfer coefficients for evaporation. *Physica A: Statistical Mechanics and its Applications*, 270(3-4):413–426, 1999.

[BK05] D. Bedeaux and S. Kjelstrup. Heat, mass and charge transport, and chemical reactions at surfaces. *Int. J. of Thermodynamics*, 8(1):25–41, 2005.

[BKDD07] VK Badam, V. Kumar, F. Durst, and K. Danov. Experimental and theoretical investigations on interfacial temperature jumps during evaporation. *Experimental Thermal and Fluid Science*, 32(1):276–292, 2007.

[Bon04] M. Bond. Non-equilibrium evaporation and condensation. Master's thesis, University of Victoria, 2004.

[BS04] M. Bond and H. Struchtrup. Mean evaporation and condensation coefficients based on energy dependent condensation probability. *Physical Review E*, 70(6):061605, 2004.

[EMS97] IW Eames, NJ Marr, and H. Sabir. The evaporation coefficient of water: a review. *International journal of heat and mass transfer*, 40(12):2963–2973, 1997.

[FW99a] G. Fang and CA Ward. Examination of the statistical rate theory expression for liquid evaporation rates. *Physical Review E*, 59(1):441, 1999.

[FW99b] G. Fang and CA Ward. Temperature measured close to the interface of an evaporating liquid. *Physical Review E*, 59(1):417, 1999.

[GBSK07] J. Ge, D. Bedeaux, JM Simon, and S. Kjelstrup. Integral relations, a simplified method to find interfacial resistivities for heat and mass transfer. *Physica A: Statistical Mechanics and its Applications*, 385(2):421–432, 2007.

[GKB+07] J. Ge, S. Kjelstrup, D. Bedeaux, JM Simon, and B. Rousseau. Transfer coefficients for evaporation of a system with a lennard-jones long-range spline potential. *Physical Review E*, 75(6):061604, 2007.

[JB04] E. Johannessen and D. Bedeaux. The nonequilibrium van der waals square gradient model.(iii). heat and mass transfer coefficients. *Physica A: Statistical and Theoretical Physics*, 336(3-4):252–270, 2004.

[JB06] E. Johannessen and D. Bedeaux. Integral relations for the heat and mass transfer resistivities of the liquid-vapor interface. *Physica A: Statistical Mechanics and its Applications*, 370(2):258–274, 2006.

[KB08] S. Kjelstrup and D. Bedeaux. Heat and mass transfer across phase boundaries: Estimates of coupling coefficients. *AAPP— Physical, Mathematical, and Natural Sciences*, 86(0), 2008.

[KK03] S. Kjelstrup and G.M. Koeijer. Transport equations for distillation of ethanol and water from the entropy production rate. *Chemical engineering science*, 58(7):1147–1161, 2003.

[MS01] R. Marek and J. Straub. Analysis of the evaporation coefficient and the condensation coefficient of water. *International journal of heat and mass transfer*, 44(1):39–53, 2001.

[ORK02] M.L. Olivier, J.D. Rollier, and S. Kjelstrup. Equilibrium properties and surface transfer coefficients from molecular dynamics simulations of two-component fluids. *Colloids and Surfaces A: Physicochemical and Engineering Aspects*, 210(2-3):199–222, 2002.

[RFB+00] A. Røsjorde, DW Fossmo, D. Bedeaux, S. Kjelstrup, and B. Hafskjold. Nonequilibrium molecular dynamics simulations of steady-state heat and mass transport in condensation : i. local equilibrium. *Journal of colloid and interface science*, 232(1):178–185, 2000.

[RKBH01] A. Røsjorde, S. Kjelstrup, D. Bedeaux, and B. Hafskjold. Nonequilibrium molecular dynamics simulations of steady-state heat and mass transport in condensation. ii. transfer coefficients. *Journal of colloid and interface science*, 240(1):355–364, 2001.

[SBK+06] JM Simon, D. Bedeaux, S. Kjelstrup, J. Xu, and E. Johannessen. Interface film resistivities for heat and mass transfers integral relations verified by non-equilibrium molecular dynamics. *The Journal of Physical Chemistry B*, 110(37):18528–18536, 2006.

[War02] CA Ward. Liquid-vapour phase change rates and interfacial entropy production. *Journal of Non-Equilibrium Thermodynamics*, 27(3):289–303, 2002.

[WF99] CA Ward and G. Fang. Expression for predicting liquid evaporation flux: Statistical rate theory approach. *Physical Review E*, 59(1):429, 1999.

[XKB+06] J. Xu, S. Kjelstrup, D. Bedeaux, A. Røsjorde, and L. Rekvig. Verification of onsager's reciprocal relations for evaporation and condensation using non-equilibrium molecular dynamics. *Journal of colloid and interface science*, 299(1):452–463, 2006.

Table of notations

		Main variables of the system
e	J	Internal energy of the gas phase
E	J	Internal energy of liquid-vapour overall
n	mol	Quantity of matter in the gas phase
N	mol	Total quantity of matter
z	m	Height of the system
		Other thermodynamic magnitudes
T_i	K	Temperature of phase i
P_g	Pa or bar	Pressure of the gas phase
b	m	Height of the liquid
ρ_i	kg m^{-3}	Mass density of phase i
μ_i	J mol^{-1}	Chemical potential of the phase i (see (2.17))
$\mathcal{E}^i$	J mol^{-1}	Molar internal energy of phase i
$\mathcal{H}^i$	J mol^{-1}	Molar enthalpy of phase i (see (1.4))
		Constants
R	J mol^{-1} K^{-1}	Gas constant
$\mathcal{L}_{\text{vap}}$	J mol^{-1}	Latent heat of evaporation
$\mathcal{C}_i$	J mol^{-1} K^{-1}	Heat capacity at constant volume of phase i
$\mathcal{M}$	kg mol^{-1}	Molar mass
$P_{\text{sat}}(T)$	Pa or bar	Vapour pressure function (see (1.3))
A, B, C	∅, K, K	Antoine's law constants for P_{sat} (see (1.3a))
		Liquid-vapour exchanges
Φ_μ	mol m^{-2} s^{-1}	Flux of matter exchanged between the two phases
Φ_q	J m^{-2} s^{-1}	Flux of energy between the two phases (see (2.9))
L_{ij}	see (2.22)	Transfer coefficients (see (2.13), (2.20) and 2.6)
R_{ij}	id.	Resistances (see (2.8))
σ	∅	Evaporation coefficient (see (2.23) and A.1)
		Piston dynamic
M_{piston}	kg	Mass of the piston
v_0	m s^{-1}	Initial speed of the piston
$P_u(z)$	Pa or bar	Function of pressure above the piston (see (4.3))
a	∅	Aspect ratio (id.)
		Dimensionless variables
ϵ	∅	Dimensionless internal energy of the gas (see (4.4))
η	∅	Dimensionless total internal energy (id.)
ν	∅	Dimensionless quantity of gas (id.)
ζ	∅	Dimensionless height of the system (id.)
υ	∅	Dimensionless speed of the piston (id.)
κ_i, Λ, S, Ω_k	∅	Numbers without dimensions (see (4.5))

List of Figures

List of Tables